4-Hydroxyphenylpyruvate Dioxygenase and Its Inhibition in Plants and Animals: Small Molecules as Herbicides and Agents for the Treatment of Human Inherited Diseases

4-Hydroxyphenylpyruvate dioxygenase and its inhibition in plants and animals: small molecules as herbicides and agents for the treatment of human inherited diseases

Journal:	*Journal of Medicinal Chemistry*
Manuscript ID	jm-2016-01395k.R4
Manuscript Type:	Perspective
Date Submitted by the Author:	n/a
Complete List of Authors:	Santucci, Annalisa; University of Siena, Italy, 1. Università degli Studi di Siena, Dipartimento di Biotecnologie, Chimica e Farmacia Bernardini, Giulia; University of Siena, Department of Molecular Biology Braconi, Daniela; Università degli Studi di Siena, Dipartimento di Biotecnologie Petricci, Elena; University of Siena, 1. Università degli Studi di Siena, Dipartimento di Biotecnologie, Chimica e Farmacia Manetti, Fabrizio; Università degli Studi di Siena, Dipartimento di Biotecnologie, Chimica e Farmacia

4-Hydroxyphenylpyruvate dioxygenase and its inhibition in plants and animals: small molecules as herbicides and agents for the treatment of human inherited diseases

Annalisa Santucci, Giulia Bernardini, Daniela Braconi, Elena Petricci, Fabrizio Manetti*

Dipartimento di Biotecnologie, Chimica e Farmacia, via A. Moro 2, I-53100 Siena, Italy. Phone: +39 0577 234330, Fax: +39 0577 234254, email: fabrizio.manetti@unisi.it

Abstract: This review mainly focuses on the physiological function of 4-hydroxyphenylpyruvate dioxygenase (HPPD), as well as on the development and application of HPPD inhibitors of several structural classes. Among them, one illustrative example is represented by compounds belonging to the class of triketone compounds. They were discovered by serendipitous observations on weed growth and were developed as bleaching herbicides. Informed reasoning on nitisinone (NTBC, **14**), a triketone that failed to reach the final steps of the herbicidal design and development process, allowed it to become a curative agent for type I tyrosinemia (T1T), and to enter clinical trials for alkaptonuria. These results boosted the research of new compounds able to interfere with HPPD activity to be used for the treatment of the tyrosine metabolism-related diseases.

1. Introduction

4-Hydroxyphenylpyruvate dioxygenase (HPPD) is an iron-dependent non-heme oxygenase involved in the catabolic pathway of tyrosine (Tyr), with very different roles in prokaryote organisms, plants, and animals. In the last four decades, a significant number of HPPD modulators has been discovered in the field of agrochemicals for weed control. In this context, an in deep analysis of the HPPD inhibitor activity and mechanism of action led to recycle a triketone compound originally designed as herbicide as a drug for the cure of human T1T.[1]

Drug repositioning (also known as redirecting, repurposing, and reprofiling),[2,3] which is the identification and development of new uses for existing drugs, has been widely applied within the drug development process.[4] In most cases, it was based on pure serendipity (one classic success story is represented by sildenafil, initially studied as an anti-angina agent and currently used to treat erectile dysfunction), while in a limited number of cases it was the consequence of an informed reasoning.[5,6]

Drug repositioning is currently a widespread approach often described in the most recent scientific literature.[3,7] It was adopted by important research centres [8,9] and the main driver for establishing novel companies,[10] journals,[11] and conferences[12] specifically addressing this topic. As a striking example, a recent paper describing the use of molecular modeling and docking simulations for repositioning 2,4-dichlorophenoxy acetic acid (a plant hormone belonging to the auxin class) as a potential anti-inflammatory agent able to inhibit the COX-2 enzyme can be cited.[13]

One of the compounds reviewed in this paper represents a classic example of reasoned repurposing of an active ingredient. This examples dates back to the eighties, well before coining of the concept of “drug repositioning”. In those years, triketones were identified as corn-selective

herbicides. Further investigations of such compounds in terms of toxicology and mechanism of action allowed HPPD (the second enzyme involved in the Tyr metabolism pathway, Figure 1) to be identified as the molecular target.[14] Based on the ability of triketones to block HPPD, a brilliant intuition arose to use 2-[2-nitro-4-(trifluoromethyl)benzoyl]cyclohexane-1,3-dione (nitisinone, NTBC, **14**, a triketone, Figure 10) to treat T1T,[1] a fatal disease caused by inactivity of the fumarylacetoacetate hydrolase (FAH, an enzyme downstream of HPPD itself, Figure 1).[15] Since the disease is characterized by the accumulation of toxic metabolites as a consequence of FAH dysfunction (Figure 28), the upstream blocking of HPPD avoids the production of such toxic metabolites.

Besides its use in T1T, **14** recently accessed clinical trials for alkaptonuria (see below), a disease due to dysfunction of homogentisate dioxygenase (HGD, another enzyme within the Tyr metabolic pathway, Figure 1). In this case, inactivity of HGD results in accumulation of 2,5-dihydroxyphenylacetic acid (homogentisic acid, HGA, **2**, an intermediate of the pathway) that undergoes oxidation and polymerization (Figure 9), fixation on cartilages and other tissues, with consequent invalidating outcomes.[16] By inhibiting HPPD, **2** cannot be further accumulated in alkaptonuria patients treated with **14**.

Finally, **14** could be potentially used in hawkinsinuria, a disease where HPPD mutations cause the production of hawkinsin (Figure 7), an unusual amino acid that is responsible for disease symptomatology.

All of the above considerations show that relocation of **14** from the agrochemical to the medical field can be considered a unique case of drug repositioning: a single drug targeting a specific enzyme could be now used to treat two (T1T and alkaptonuria) or perhaps three (if hawkinsinuria is included) human diseases.

The important role played by triketones and structurally different HPPD inhibitors led many research groups from both academy and pharmaceutical/agrochemical companies to design, synthesize, and test many additional compounds to find new modulators of HPPD activity. The aim of the present review is to describe such efforts. In particular, structural and functional properties of HPPD as well as the involvement of the enzyme in human diseases are described in the first paragraphs. Then, a literature survey is presented to summarize and describe the various classes of compounds able to interfere with HPPD activity, providing structural requirements and pharmacokinetics parameters.

2. The enzymatic pathway

Since its discovery, HPPD has been gaining crucial importance due to its involvement both in human hereditary diseases and biosynthesis of UV shields necessary for chlorophyll protection in plants.

In humans, HPPD is a key enzyme within the catabolic pathway Tyr that begins with the hydroxylation of natural phenylalanine (Phe) and proceeds with its degradation to small anionic species, such as acetoacetate and fumarate (Figure 1). During the first step, Phe is hydroxylated at the *para*-position by the Fe(II)-dependent phenylalanine-4-hydroxylase (PAH) in the presence of oxygen and tetrahydrobiopterin as cofactor to yield Tyr. In the next step, a reversible reaction catalyzed by the Tyr aminotransferase (TAT, a transaminase) converts Tyr into 4-hydroxyphenylpyruvate (HPP, **1**), in the presence of 2-oxoglutarate as co-substrate and pyridoxal 5'-phosphate as cofactor. Compound **1** is then transformed into **2** by HPPD. An additional iron-dependent dioxygenase (HGD) is responsible for the ring-opening reaction to 4-maleylacetoacetate, which then undergoes a *cis-trans* reversible isomerization, catalyzed by the

glutathione-dependent maleylacetoacetate isomerase (MAAI), to yield 4-fumarylacetoacetate. In the last step of the pathway, fumarylacetoacetate is hydrolyzed into acetoacetate and fumarate by FAH, a Ca/Mg-dependent hydrolase.

3. The enzyme HPPD

HPPD (EC 1.13.11.27) belongs to the class of α-keto acid-dependent oxygenases that have only two substrates: **1** (either as the source of α-keto acid or the small molecule where the reactions of the catalytic cycle occur) and molecular oxygen. They differ from the majority of α-keto acid-dependent oxygenases that requires α-ketoglutarate as the source of α-keto acid and an additional substrate to be processed, in addition to oxygen molecules.[17,18]

3.1. Human HPPD: isoforms and mutations

HPPD is an oxidoreductase with dioxygenase activity that catalyzes the third step of the catabolic pathway of Phe and Tyr, consisting in the oxidation of **1** to **2**. In humans, HPPD is characterized by a 393 amino acid sequence (entry P32754[19] of the UniProt Knowledgebase database - UniProtKB/Swiss-Prot).[20] Two isoforms produced by alternative splicing have been described: the full length isoform 1 (392 amino acids, missing Met1; numbers are according to the 393 amino acid sequence P32754[19] of the human HPPD) and the truncated isoform 2 with the sequence 1-39 of missing residues. At least 5 modified amino acids have been described: three phosphoserines (211, 226, and 250), one *N*6-succinyllysine (132), and an *N*-acetylthreonine (2). Natural variants involved in type III tyrosinemia (namely, Ala33Thr, Tyr160C, Ile267Phe, Ala268V, Ile335Met, and Val340Leu), hawkinsinuria (namely, Ala33Thr, Asn241Ser, and Ala268V), or not yet correlated to any disease (namely, Arg113Gln), have been described. A metal binding site containing an iron ion as the cofactor is constituted by His183, His266, and

Glu349. The last amino acid is critical for catalytic activity of HPPD. In fact, while metal coordination could be guaranteed by the two His residues, variants at the Glu349 residue only show a 5-10% residual activity at maximum.[21]

3.2. Multiple sequence alignment

Among about half a million sequences of the reviewed section of the UniProtKB/Swiss-Prot, 28 sequences (Table 1) have been described as belonging to the HPPD enzyme. Multiple sequence alignment performed on them with Clustal Omega at the Protein Information Resource (PIR) web site[22] showed that 18 out of the 44 (41%) conserved amino acid residues are contouring the Fe(II) binding site (Supporting Information, Table S1): Asp182, His183 (catalytic triad), Gln265, His266 (catalytic triad), Ala268, Leu332, Leu333, Gln334, Phe336, Phe347, Glu349 (catalytic triad), Ile351, Gly358, Phe359, Gly360, Gly362, Asn363, Phe364. This suggests a high structural similarity among the iron-containing HPPD binding sites from various sources.

3.3. Three-dimensional structures of holo-HPPD and HPPD-inhibitor complexes

Despite the high structural similarity showed at the level of the binding site, HPPDs from various organisms differ for their oligomeric state. In fact, HPPD from mammals,[23] plants,[24] and *Streptomyces avermitilis*[25] are homodimers, while the *Pseudomonas fluorescens* HPPD (*Pf*HPPD) is organized in homotetramers.[26] Moreover, the monomer surfaces responsible for the formation of dimers and tetramers are different in plant and bacterial enzymes.[24] Significant differences have been also found at the level of single monomers. As an example, the C-terminal α-helix H11 of *Zea mais* HPPD (*Zm*HPPD) is interposed between the solvent and the active site, while a 60 degrees rotation of the same helix exposed the *Arabidopsis thaliana* HPPD (*At*HPPD) binding site to the solvent.[24] A similar conformational rearrangement of the C-terminal α-helix

(namely, a rotation of about 40 degrees) was found in the complex between *Streptomyces avermitilis* HPPD (*Sa*HPPD) and **14**, in comparison to the *Pf*HPPD.[25]

The Protein Data Bank (RCSB PDB)[27] collects 12 3D structure of HPPD from different organisms (prokaryotes, plants, and mammals, Table 2). All of them have been determined by X-ray crystallographic studies and showed a different coordination sphere of their iron cofactor. Six of the PDB entries describe HPPD in its holoenzymatic form. Unfortunately, the structure of the complex between HPPD and its natural substrate **1** or one of its reaction intermediates and transition states is not available yet neither from experimental sources nor from theoretical calculations. However, the 3D structures of six complexes between HPPD and small molecule inhibitors are available which contain a pyrazole [(namely, **3** (DAS869),[28] and **4** (DAS645),[23] Figure 2)] or a triketone (namely, **14** and sulcotrione **15**, Figure 10) inhibitor (Table 2). None of them is from a human source.

3.4. HPPD-inhibitor interactions

An analysis of the graphical representation of the co-crystallized HPPD-inhibitor complexes provides a detailed description of the interaction pattern between the inhibitor and the HPPD binding site. The C-terminal domain of the enzyme (Gln375 seems to be critical in humans)[29] harbor a wide cavity exposed to the solvent that accommodates the iron ion cofactor. Iron coordination is fulfilled by the usual amino acids (two His and a Glu), while the remaining coordinating water molecules are replaced by the β-keto-enol system found either in the pyrazole and triketone inhibitors. While both **14**[30] and the diketonitrile of isoxaflutole (**24**, Figure 11)[31] were described to bind the complex between HPPD and ferrous ion, within the co-crystal structure between HPPD and pyrazole inhibitors neither the metal ion at the binding site (iron or cobalt) nor its oxidation state (+2 or +3) can be distinguished.[23] On the contrary, X-ray

crystallography confirmed that **14** binds to the ferrous/HPPD system,[25] while the cofactor of the HPPD-**15** complex is reported in its ferric form (Table 2).

*3.5. Comparison of the complexes between the pyrazole **3** and HPPD from different organisms*

A superposition was performed by the Superimpose Proteins tool (provided by the Discovery Studio 3.0 Visualizer software)[32] between the two complexes (namely, 1SQI from *Rattus norvegicus* and 1TFZ from *Arabidopsis thaliana*) containing the same pyrazole inhibitor **3** (Figure 3). A very similar binding mode of the inhibitor was found (308 residues with a 1.2 Å root mean square deviation, rmsd, on Cα atoms), consequent to the fact that all of the amino acids in the binding site were conserved residues, although the entire sequences showed only a 29% amino acid identity. In particular, apart the interactions that involve the β-keto-enol system of the pyrazole ring, additional complex stability arose from various π-π interactions involving the aromatic portion of Phe residues and the phenyl rings of the inhibitor. Hydrophobic contacts were also found between the N-*t*Bu group of the inhibitor and a Pro residue. Unexpectedly, no hydrogen bonds and ionic interactions involving the inhibitor were found for complex stabilization.

3.6. Comparison of the complexes between AtHPPD and different pyrazole inhibitors

An expected better superposition (362 residues with a 0.3 Å rmsd, Figure 4) was found between two structures from *A. thaliana* (namely, 1TFZ and 1TG5) with different pyrazole inhibitors (namely, **3** and **4**). The usual interactions with the iron ion and with the aromatic portions of the inhibitor were maintained, without any hydrogen bond. The major difference was due to the 115 degrees rotation of the Phe403 side chain induced by the presence of the 2,4-dichlorophenyl group of **4**. Such a conformational rearrangement, together with a significant displacement of a Pro residue and to the flexibility of the C-terminal helix, accounted for the 12 nM inhibitory

activity of **4** toward *At*HPPD, and for the inability of the same compound to inhibit the rat enzyme that can not undergo these structural changes.[23] Compound **4** has been discovered within a campaign for the identification of plant-selective HPPD inhibitors, starting from a small database (about 1000 entries of the Dow AgroSciences library) of HPPD inhibitors. Selectivity of such a compound was attributed to the presence of its N1-*t*Bu and C3-phenyl substituents which were identified as common structural features for plant selectivity. These chemical groups induce the Pro displacement and the Phe conformational rearrangement that are allowed only in *At*HPPD, while they are not possible in HPPDs from other species, such as *Rattus norvegicus* HPPD (*Rn*HPPD).[23]

*3.7. Comparison of the complexes between the triketone **14** and HPPD from different organisms*

A comparison between HPPD structures in complex with **14** (5CTO from *A. thaliana* and 1T47 from *S. avermitilis*) resulted in a very similar orientation of the inhibitor within the enzyme binding site (314 residues with a 1.1 Å rmsd, Figure 5). Compound **14** was able to give parallel stacked π-π interactions with the Phe residues and hydrophobic contacts between the CF_3 substituent and Leu residues. In the case of 1T47, a nitro-π stacking between the nitro group and Phe336 was also possible, the distance between the centroid of the amino acid phenyl ring and the nitro nitrogen atom being 3.8 Å, in agreement with those reported in the literature (ranging from 3.58 to 5.08 Å).[33] Hydrogen bonds between the inhibitor and the enzyme were not detected. Importantly, EPR studies demonstrated that **14** gave a very tight binding to ferrous ion that avoided iron oxidation by dioxygen molecules (O_2), thus permitting crystallization of the HPPD-Fe(II)-inhibitor complexes under aerobic conditions.[30] The stability of the triketone/HPPD complexes is very high, with K_d values in the picomolar range and a complex dissociation half-time in the hour or day range. For these properties, such compounds have been reported as

irreversible inhibitors,[30] even though reversion of triketone binding, with consequent reactivation of HPPD, has been demonstrated.

4. The catalytic reaction

The 3D structure of HPPD in its resting state shows a ferrous ion bound to an amino acid triad made of two His and one Glu, while water molecules (or an acetate ion in the case of 1CJX) complete the coordination sphere of the metal into various architectures (i.e., tetrahedral, trigonal bipyramidal, squared pyramidal, octahedral, Table 2). In several cases, the functional iron ion was replaced by Co(II) ions by using cobaltous chloride under crystallization conditions (i.e., 5EC3, 1ISQ).

The overall catalytic reaction mechanism leading from the Fe(II)-HPPD/**1** adduct to **2** was studied with theoretical calculations supported by previous experimental data.[34-37] Three major consecutive steps were identified (Figure 6), consisting of: 1) decarboxylation of **1** to the corresponding acetic analogue (upon binding of the substrate to the ferrous ion and reaction with the dioxygen species); 2) hydroxylation of the phenyl ring; and 3) migration of the acetic side chain to the adjacent position with production of **2**.

In the first step of HPPD biocatalysis (Figure 6), it was hypothesized that the Fe(II)-HPPD/**1** adduct is attacked by a dioxygen molecule to yield a ferric superoxide anion radical which rearranges into a peracid intermediate *via* oxidative decarboxylation of the α-ketoacid with release of CO_2. Opening of the four-membered ferrous adduct by heterolytic cleavage of the peroxide bond results in a potent oxidant phenylacetic intermediate containing a Fe(IV)-oxo species. The latter is responsible for an electrophilic attack on position 1 of the phenyl ring with consequent de-aromatization and formation of a ring radical σ complex. This is the rate-limiting

reaction of the catalytic pathway. Cleavage of the C1-C_{acetic} bond leads to re-aromatization and generation of an instable biradical intermediate that initiates the hydroxylation in position 1 and the peculiar migration of the acetic side chain to position 2 of the ring. For this purpose, the 4-hydroxy-cyclohexandienone undergoes tautomerization (by a direct proton transfer mediated by the carboxyl group and without any contribution from the solvent)[34] and to re-aromatization. The resulting final product is the complex between HPPD, the Fe(II) cofactor, and **2**.

Alternative rearrangements of the ring radical σ complex or the Fe(IV)-oxo intermediate leading to an arene oxide were hypothesized as well (Figure 7). For engineered HPPD (P214T and F337I mutants of *Pseudomonas fluorescens* strain P.J. 874), a rearrangement of arene oxide into an oxepine derivative further evolving by tautomerization into the corresponding oxepin-5-one was suggested.[38] Alternatively, opening of the epoxide ring of the arene oxide or a rearrangement of the ring radical σ complex could yield the quinolacetate that reacted with cysteine residues by Michael addition, giving hawkinsin in N245S mutant of *S. avermitilis*.[39]

Several steps of the HPPD catalytic cycle are still experimentally inaccessible, and only a few reactive intermediates have been identified so far. Hence, alternative mechanistic hypotheses involving different intermediate chemical species from those reported in Figure 6 and 7 were proposed by means of computational studies.[40] An in depth analysis of HPPD, both in terms of structure, complex formation, and catalytic cycle has been recently published.[17,18,35,41]

5. The fate of HGA in plants and mammals

Fate of **2** differs in plants and humans. In plants (Figure 8),[42] following an anabolic pathway, **2** is first decarboxylated, then nonaprenylated at position 3 to give 2-methyl-6-nonaprenyl-1,4-benzoquinone (MNPBQ, **5**), and finally methylated at C6 to yield plastoquinol-9 (also referred to

as plastoquinone in its diketo form). Importantly, the plastoquinol/plastoquinone redox system is involved in the photosynthetic electron transport chain that allows for phytoene desaturase-mediated oxidation of phytoene to carotenoids.[43] On the basis of this pathway, inhibition of pigment biosynthesis by repression of the HPPD activity and production of **2** results in photodestruction of chlorophyll and whitening of plant tissues (the bleaching effects).

Alternatively, **2** can be first decarboxylated, then phytylated at position 3 to give 2-methyl-6-phytyl-1,4-benzoquinone (MPBQ, **6**). Ring closure and a subsequent methylation at C5 yields δ- and β-tocopherol, respectively. On the other hand, methylation of **6** at C3 produces the corresponding dimethyl derivative 2,3-dimethyl-6-phytyl-1,4-benzoquinone (DMPBQ) that undergoes ring closure and subsequent methylation at C5 yielding γ- and α-tocopherol, respectively.

Chemical reactivity of **2** seems to be different as well. It is reported as the main phenolic compound with significant antioxidant activity in Sardinian "bitter honey" (a monofloral honey from *Arbutus unedo*, Ericaceae).[44] In fungi and bacteria, **2** undergoes oxidation and polymerization into pyomelanin, which serves as protection from sunlight and oxidative attack by host cells.[45-47] Conversely in humans, where **2** is accumulated upon mutations of HGD, **2** shows an outstanding propensity to oxidation into the corresponding quinone (Figure 9) with generation of ROS and polymerization into a black substance referred to as ochronotic pigment, not well defined in terms of composition and structure. Urine blackening and deposition of black pigments in cartilage, epidermis, and sclera are typical of an autosomal recessive human disease known as alkaptonuria.[16]

6. Evaluation of HPPD catalytic activity

HPPD catalytic activity can be evaluated through different assays, as follows:

1) Monitoring the formation of a complex between the enol form of **1** with orthoboric acid which absorbs at 308 nm.[48]

2) Monitoring the production of **2**.[49] For instance, Dayan and co-workers overexpressed recombinant HPPD from *A. thaliana* in *E. coli* and treated the cell-free extract with various concentrations of HPPD putative inhibitors together with the natural HPPD substrate **1**. The reaction was stopped after 15 min and the amount of **2** was quantified by HPLC (detection based on UV absorbance at 288 nm). Changes in oxygen consumption during HPPD-dependent reaction on **1** were monitored as well.

3) Monitoring changes in dissolved oxygen concentration over the time by using Clark electrode or SensorDish technology. For instance, rat liver homogenates could be used as the source of HPPD whose activity could be inferred by monitoring either the uptake of molecular oxygen or the release of $^{14}CO_2$ from a [^{14}C]-labeled substrate.[50-52]

7. Activity of HPPD inhibitors and their selectivity in plants

Although the amino acids that constitute the HPPD binding site are conserved among various species, there are inhibitors that show selectivity toward enzyme from plants or animals. One of the reasons of this selectivity could be ascribed to significantly different K_d values: differences of two or more orders of magnitude correspond to slight differences in energy and are not easily perceivable by structural analysis of the HPPD/inhibitor complexes. Another important parameter to be considered for selectivity is the duration of biological action, expressed in terms of residence time (defined as $1/K_{off}$) of the inhibitor within the HPPD binding site.[53] Additional factors could also contribute to inhibitor selectivity. As an example, selectivity of mesotrione (**16**,

an HPPD inhibitor belonging to the triketone class, Figure 10) for maize is mainly attributable to the higher potency of this compound toward dicotyledonous plants in comparison to monocotyledons (such as the same maize), as well as to the fact that foliar uptake of the herbicide is slower in maize than in other plants. However, the rapid metabolism by maize seemed to be the most significant parameter for selectivity of **16**.[54] The distinction between selective and non-selective HPPD inhibitors lost its importance when genetically-modified and herbicide-tolerant crops able to resist to non-selective compounds (such as glyphosate) were selected. An additional example was a transgenic soybean that was designed with an optimized HPPD to become resistant to triketones (namely, **16** and tembotrione, **17**, Figure 10), as well as to isoxaflutole (**23**, Figure 11). Also in this case, the known selectivity of HPPD inhibitors toward maize crops was overridden by a certain number of mutations that rendered the soybean insensitive to such compounds.[55]

8. Timeline of HPPD inhibitors marketed as herbicides

The story of small molecules acting as HPPD inhibitors and marketed as bleaching herbicides began during the eighties with benzoylpyrazoles such as pyrazolynate (**7**), pyrazoxyfen (**8**), and benzofenap (**9**, Figure 10).[56-58] In the nineties, the first triketone (**15**) was commercially available, followed by the first isoxazole compound (**23**). In the next decade, **16**, benzobicyclon (**21**), **17**, and tefuryltrione (**18**) were marketed among the triketones, while topramezone (**12**) and pyrasulfotole (**13**) belong to the pyrazole class. Recently, an additional triketone (namely, bicyclopyrone **19**) has been registered in the USA as a pesticide for the treatment of corn.[59] Moreover, fenquinotrione (**20**) and the pyrazole prodrug tolpyralate (**10**) are under development for weed control in rice and in corn, respectively.[60]

Studies on HPPD inhibitors will probably increase in the next years because of the onset of resistant weeds. Since 2009 at least two species of *Amarantus* (Amaranthaceae) have been found to be resistant to HPPD inhibitors in the USA.[61] This means that new active ingredients able to selectively inhibit the growth of weeds at low concentrations will be required in the near future.

Several of the currently available HPPD inhibitors are prodrugs (in the field of agrochemicals they are referred to as procides, that is pro-herbicides) that need to be transformed into the corresponding active ingredients to chelate iron ions of the HPPD binding site. As an example, 4-benzoyl-5-aryl-pyrazoles undergo degradation (by hydrolysis in water or in plants, as well as by microbial activity) that affects the C5-pyrazole substituent to yield the common 4-benzoyl-5-hydroxy-pyrazole as the active compound (Figure 10).[62-63] In a similar way, **21** is transformed into the corresponding active triketone derivative **22** by a base-catalyzed nucleophilic addition with consequent release of the thiophenolate anion.[64-65] Finally, **23** shows HPPD inhibitory activity upon isoxazole ring opening to the linear diketonitrile **24** (Figure 11).[66]

9. Small molecules as inhibitors of HPPD: triketones

9.1. Serendipitous discovery of triketones as HPPD inhibitors

The story of HPPD inhibitors began with the serendipitous observation that the growth of plants and weeds in the field area under the red bottlebrush plant (*Callistemon citrinus*, Myrtaceae) was strongly disfavored in comparison to the adjacent parts of the field.[67] It was immediately clear that neither the shade created by the bottlebrush plant nor its litterfall were responsible for growth inhibition of other plants. Thus, the presence of allelopathic substances in the soil was hypothesized to account for the suppression of plant growth. To check for this hypothesis, samples of soil under the bottlebrush plant were submitted to solvent extractions and the resulting

fractions were assayed for their herbicidal activity. The sole fraction that showed a significant bleaching activity on the emerging plants contained an active ingredient later identified as the isovaleryl syncarpic acid, an already known compound previously named as leptospermone (**26**, Figure 12) for its occurrence in the essential oils of the *Leptospermum flavescens* (Myrtaceae).[68] Similar results were obtained starting from fresh leaves of *C. citrinus*. Although **26** was demonstrated to be an allochemical agent,[69] the possibility to transform it or one of its derivatives into an herbicide was however unrealistic mainly because of its weak activity. As a consequence, studies on these compounds were discontinued.

*9.2. Additional triketones from natural sources: congeners of **26***

In addition to *Callistemon* spp., other Australasian Myrtaceae were found to produce β-triketones. As an example, the steam distilled oil of *Leptospermum scoparium* (Myrtaceae, also referred to as essential oil of manuka), in addition to the already known **26**, also contains a series of its derivatives with different hydrophobic chains attached at the *exo*-carbonyl group.[70] Among them, grandiflorone (**27**, Figure 12) showed an IC_{50} value (measured as changes in oxygen consumption to convert **1** to **2**) toward *At*HPPD about three-fold higher than that of **15** (750 vs 250 nM, respectively), while significantly better than that of **26** (750 vs 11800 nM, respectively, 15-fold more active).[49,71] Interestingly, introduction of a long alkyl chain (a nonyl group as in **28**) led to a 19 nM activity. Accordingly to a previous hypothesis suggesting that the nature of the binding to HPPD was dependent from the substituent at position 2 of the cyclohexandione ring,[50,51] these naturally-occurring compounds and their derivative were time-independent competitive reversible inhibitors due to the fact that they had a 2-alkyl (**26** and the nonyl derivative **28**) or 2-phenetyl moiety (**27**). Differently, synthetic compounds bearing a electron-deficient aromatic ring (i.e., bearing electron-withdrawing substituents at the *ortho*-position and, preferably, also at the

para-position) usually resulted to have a tight binding toward HPPD to be considered as irreversible inhibitors.[50,51] The high activity of **28** was impossible to account for by a simple relationship between IC_{50} and compound lipophilicity. However, a CoMFA study on these triketones showed that the steric properties of the compounds contributed for 66% activity, while only 34% was due to the electrostatic components.[71] This model accounted for the high activity of the nonyl derivative **28**. In fact, a region of the space identified by the model as profitable for activity was occupied by the terminal edge of the linear alkyl chain. Moreover, docking simulations showed that the same linear appendage was accommodated within a lipophilic pocket of the *At*HPPD binding site. Unfortunately, although their availability in large amounts from natural sources, these compounds showed poor pharmacokinetic parameters in comparison to those found for commercially available triketones obtained by SAR optimization and synthesis. Because of their limitation, naturally-occurring compounds similar to **26** and their derivatives were not further profiled.

9.3. *The benzoyl-cyclohexanedione core discovered as a reaction by-product*

Serendipity was further invoked when, in the attempt to synthesize sethoxydim (**29**) derivatives as herbicide agents (Figure 13), the benzoyl dimedone derivative **30** was obtained as by-product of the synthesis pathway. Subsequent structural optimization by small changes at both the cycles led to very active compounds and laid the foundation for SAR (Figure 14), thus suggesting that an electron withdrawing group at position 2 of the phenyl ring is fundamental for activity.[72] In particular, such a substituent should carry out two tasks at the same time:[73] rendering the phenyl ring an electron deficient moiety able to interact by π-π stacking with aromatic amino acids of the HPPD binding site, and blocking position 2 thus avoiding an intramolecular cyclization to the corresponding dihydroxanthone (Figure 15). In alternative, an undisplaceable non-electron

withdrawing group (such as a methyl) could occupy position 2, while another electron withdrawing moiety should be placed preferably at position 4 of the phenyl ring. Overall, the ability of the substituents at both positions 2 and 4 to render the aromatic ring an electron-deficient moiety is also related to the acidity of the molecule, the enol tautomer of triketones being the vinylogue of the benzoic acid. On such bases, more electron-withdrawing substituents at the phenyl ring are responsible for higher acidity of the compound. Finally, introduction of alkoxy groups at the *meta*-position resulted in further increased activity toward HPPD. The hypothesis that a pocket able to accommodate such substituents could be present in the protein was next confirmed by X-ray structures of the HPPD/**14** complexes (5CTO and 1T47) where it is clear that the substituent at the *meta*-position could be located within a cavity accessible to the solvent.[56]

Combining structural optimization and taking into account herbicidal selectivity (in part dependent from different metabolism among plants) and soil persistence, **15** was the first triketone derivative to be commercially available as maize selective herbicide. It was followed by **16**, whose registered name (Callisto) was reminiscent of *Callistemon*. Compound **16** was found to be about 100-fold more active than **26** in pre- and post-emergence treatments, and showed broad activity and excellent maize selectivity. Further attempts to modulate soil persistence, crop selectivity, and animal toxicology led to the discovery of thousand additional triketones, including **14**.

9.4. Mechanism of action of triketones

9.4.1. Triketones do not inhibit phytoene desaturase. The discovery of the mechanism of action of triketones was a very challenging and fascinating task. The bleaching properties of these compounds suggested their ability to interfere with the production of plant pigments, such as

tocopherols and carotenoids which also serve to protect chlorophyll from sunlight degradation. In addition, the significant increase in phytoene concentrations upon herbicidal treatment led to the hypothesis that triketones could act at the level of phytoene desaturase (an enzyme involved in the synthesis of carotenoids), resulting in phytoene accumulation. However, in vitro activity of this enzyme was not affected by none of the triketone herbicides,[74] thus leading to the conclusion that the molecular target of these compounds was different from phytoene desaturase.

9.4.2. Triketones do not inhibit Tyr hydroxylase (TH). On the other hand, classes of TH inhibitors, sharing a common triketone structural motif, were already known as bleaching herbicides. This fact prompted the researchers to check whether **14** and congeneric compounds could act as TH inhibitors. For this purpose, a colorimetric assay showed the presence of *p*-hydroxyphenyl compounds (Tyr belongs to the same chemical class) in the urine of rats upon treatment with **14**, while a 20-fold increase in plasma Tyr concentration (from about 0.1 mM to more than 2 mM) was found in comparison to controls. Although these results were both in agreement with TH inhibition, an in vitro enzymatic assay showed that **14** was not able to inhibit directly TH activity. An in depth analysis on chemical composition of urine also showed the presence of unusually high amounts of compounds derived from Tyr metabolism, such as **1** and *p*-hydroxyphenyllactic acids. This result, combined with the fact that **1** was known to be a substrate for HPPD, led to experimental evidence that triketones act as inhibitors of rat liver HPPD.[50] In particular, studies aimed at evaluating changes in oxygen consumption by rat liver HPPD treated with triketones showed a time-dependent inhibition of the enzyme *via* a competition with the substrate **1**. Compound **14** (50 nM) was able to reduce rat liver HPPD activity by 50% in 30 sec with an IC_{50} value of about 40 nM.[50] HPPD activity was partially restored by increasing substrate levels or, by itself, over 7 h (about 13% activity recovery). Experimental evidence definitely showed that

triketones are characterized by a tight but reversible binding to rat liver HPPD,[51] with an half-life of about 63 h for **14**.

9.4.3. Triketones do inhibit HPPD and cause the bleaching effect. Identification of HPPD as the unique molecular target of triketones allowed to account for bleaching symptomatology in plants.[73] In fact, inhibition of HPPD-mediated conversion of **1** into **2** abrogates the biosynthesis of either tocopherols or plastoquinone (Figure 8). The latter compound is required for the biosynthesis of carotenoids from phytoene, mediated by phytoene desaturase. Carotenoids are required to quench light-dependent singlet oxygen that is responsible for degradation of the photosynthetic assembly and breakdown of leaf pigment (the bleaching effect). In summary, treatment of plants with triketone herbicides is responsible for HPPD inhibition and results in the so-called triketone effect,[75] consisting in a significant increase of Tyr levels and a drop of plastoquinone concentration, with the consequent appearance of leaf bleaching.

A detailed survey of literature papers and patents dealing with the discovery of triketones and their development for agrochemical purposes has been recently reported.[76]

9.5. A correlation between inhibitory activity of triketones and their keto-enol isomerization

An interesting study on the correlation between HPPD inhibitory activity of triketones and their ability to give keto-enol isomerization (Figure 16) provided experimental evidence on their mechanism of action at the level of the HPPD binding site. Triketones were already known as competitors of the natural HPPD substrate **1**. Several analogues of **14** were designed to check for the importance of the keto-enol isomerization, as well as to evaluate whether the triketone system was a mandatory structural requirement for pig liver HPPD inhibitory activity.[77] Several triketones (i.e., **31** and **32**, Figure 17), found to have a submicromolar activity (ranging from 160 to 700 nM), also returned a colored solution when treated with ferric ions, thus suggesting the

presence of free phenolic hydroxyl groups within their structure, which accounts for a keto-enol tautomerization. Moreover, both the triketo and the endo-enol forms of **14** were ruled out as a result of NMR studies, thus demonstrating that the exo-enol form was the sole tautomer present in aqueous solution at neutral pH.[30,73] This result was however in contrast with those reported by X-ray crystallographic studies,[77] NMR experiments, and theoretical simulations[78] that proposed a predominance of the endo-enol form of triketones.

X-ray crystallography clearly demonstrated that active compounds were characterized by an almost planar β-diketo system, which was required for tautomerization to occur. Additional experimental details, such as bond length and UV absorption, supported the hypothesis of an extensive conjugation within the triketone moiety. In further agreement, replacement of one of the cyclohexandione carbonyl groups of **31** (Figure 17) with a MeO substituent led to **33**, whose activity decreased by at least two orders of magnitude (from 0.16 to 52 μM, respectively), because of steric clashes that forced the cyclohexane ring out of the plane of the external carbonyl (about 60 degree dihedral angle), with a consequent loss of conjugation. These results indicate that inhibitory activity is related to the presence of a β-keto-enol system mimicking the α-ketoacid of the natural substrate in coordinating the iron ion at the HPPD binding site. Coplanarity of the external carbonyl group and the cyclohexanedione ring is also required to allow for keto-enol tautomerization. Finally, only one of the two carbonyl groups on the cyclohexane ring is necessary (**32** retained a 0.7 μM activity), while the external carbonyl is a mandatory requirement (**34** showed a 126 μM activity).

9.6. In vitro evaluation of triketones in human fibroblasts

In a recent paper, twelve triketone derivatives and **23** were assayed for their ability to inhibit rat liver HPPD activity, for their cytotoxicity toward human primary fibroblasts, and to affect

intracellular Tyr levels.[52] As a result, in addition to **16**, two benzoyl dimedone derivatives (**35** and **36**, Figure 18) showed a very interesting biological profile. Inhibition of the enzyme activity was measured on the basis of oxygen consumption and led to IC_{50} values in the two-digit nanomolar range (37, 36, and 60 nM, respectively). Cytotoxicity was quantified in a MTT assay and found to be higher than 1 mM for the three compounds at 24 and 144 h after administration. Tyr accumulation induced by **35** was about 7% lower than that found for **14** at the highest concentration tested (0.1 μM). In disagreement with previous reports on different in vitro and in vivo models, **16** caused a decrease of Tyr concentration (about 14%) at the highest dose. Although this result was ascribed to the activation of alternative pathways able to catabolyze Tyr excess (i.e., it is known that inhibition of rat HPPD by **15** is able to increase enzymatic activity of TAT),[79] in-depth studies are required to gain insight on this surprising trend.

9.7. Additional HPPD inhibitors: small molecule hybrid compounds bearing the triketone core

Starting from a benzoylcyclohexane-1,3-dione (Figure 19) as the scaffold already known to bind HPPD and to inhibit its enzymatic activity, simple substituents were used to decorate position 2 of the aromatic ring. Enzymatic activity of purified pig liver HPPD was monitored spectrophotometrically. Although electronegative group (Cl, Br, I, nitro, and CF_3) led to submicromolar inhibitory activity (from 0.16 to 0.76 μM) up to 70-fold better than the corresponding unsubstituted analogue (11 μM), these compounds were not further studied because their activity was significantly lower than that of **14** in the same assay (40 nM). On the other hand, an interesting attempt of molecular hybridization was experimented. In fact, HPPD is also known to catalyze the conversion of α-ketoisocaproate (thus bearing a diketo moiety) to β-hydroxyisovalerate in the metabolism of leucine. As a consequence, the aromatic moiety of the previous compounds was replaced by an *i*-Pr group (**37**), as found in the isocaproate, or with

linear and branched alkyl moieties. Unfortunately, the cyclopropyl derivative **38** was the sole compound that maintained a micromolar activity (6 μM), while the corresponding *i*-Pr analogue **37** was 15-fold less active (93 μM).[80,81] This difference in activity was ascribed to the different conformational properties of the cyclopropyl moiety in comparison to the structurally similar *i*-Pr group, being the first substituent blocked in a conformation characterized by the cyclopropyl plane bisected by the plane of the adjacent carbonyl group, with the *i*-Pr being free to rotate.

In a parallel way, maintaining a structural feature reminiscent of the β-diketone system, a series of cyclohex-2-en-1-one esters was designed (Figure 19).[82] Also in this case, the cyclopropyl derivative **39** was the most active compound (30 nM toward pig liver HPPD), while simple linear and branched alkyl groups were detrimental for activity, whose values spanned micromolar concentrations. Halogens at position 2 led to more active compounds (**40** and **41** with 15 and 28 nM activity, respectively), while other substituents at the same position were not tolerated.[83] Attempts to modify the cyclohexenone scaffold led to unprofitable results, with the sole exceptions of a contracted five-membered ring as in **42** or a coumarin moiety as in **43**, which maintained a 70 and 110 nM activity, respectively.

Interestingly, the 5-carboxyethyl ester of **38** (**44**), already known as an inhibitor of another non-heme Fe(II)- and α-keto acid-dependent dioxygenase (namely, GA_{20} 3β-hydroxylase, involved in the biosynthesis of gibberellins in plants), was considered as a putative good starting point for further optimization of HPPD inhibitors, because of its triketone scaffold.[84] On this basis, molecular hybridization by merging **39** and **44** led to the trisubstituted cyclohexenone **45** with a pig liver HPPD inhibitory activity comparable to that of **14** (40 nM). Such a compound and its congeners were however abandoned because both the ester moieties showed a significant liability in aqueous solution.[84]

9.7.1. Triketone-based hybrid compounds: quinazolindiones. Additional hybrid compounds were also synthesized starting from the classical triketone scaffold based on a cyclohexane ring and a quinazolindione moiety (Figure 20).[85] A SAR analysis clearly showed that compounds bearing an unsubstituted cyclohexane ring had better inhibition constants (K_i) of the *At*HPPD enzymatic activity, in the range of two-digit nanomolar concentrations. Exceptions were represented by *N*1-aryl derivatives that were about one order of magnitude less active. The most active compound (**46**) showed a three-fold higher activity compared to **16** (5 versus 13 nM, respectively). Moreover, while a mono-methyl substitution at the cyclohexane ring maintained a two-digit nanomolar activity, a *gem*-dimethyl pattern generally resulted in a decrease in activity. In order to further improve *At*HPPD inhibitory activity, a series of *N*1-methyl analogues bearing various substituents at the 5-position of the quinazoline core, at the pendant phenyl ring, as well as at the cyclohexyl ring was synthesized and tested. Many of the new compounds maintained a two-digit nanomolar activity toward *At*HPPD, although none of them was more active than **46**.[86]

9.7.2. Triketone-based hybrid compounds: quinolines. A series of very active compounds was obtained changing the quinazoline core with a quinoline ring bearing the triketone system at position 3 (Figure 20).[87] In particular, given a methyl group at position 8, the most profitable substituents were a methyl, methoxy, or cyano group at position 2 of the quinoline and a H or Me at position 5 of the cyclohexane. These compounds showed a 7-9 nM activity (expressed as K_i), better than that of **16** (13 nM). Both quinazoline and quinoline compounds were assayed for their activity as herbicides, crop selectivity, and ability to inhibit *At*HPPD in vitro, but they were not further evaluated toward human HPPD.

9.7.3. Triketone-based hybrid compounds: lengthening the aryl side chain. In the attempt to find more profitable interactions between the aryl side chain of the triketone moiety and the aromatic

residues surrounding the *At*HPPD binding site, the classical benzoyl group at the position 2 was extended by insertion of a -CH_2-O- spacer (Figure 20).[88] Many of the resulting compounds showed K_i values in the micro- or submicromolar range, one or two orders of magnitude higher in comparison to that found for **17** (13 nM). The best compounds in terms of affinity and plant selectivity were found by introduction of a methyl or chloro group at the ortho position and a electron-withdrawing substituent at the para position. Their affinity ranged between 31 and 37 nM. Interestingly, one of these compounds was described as the first HPPD inhibitor with good safety toward canola.

10. Pyrazole derivatives

Another important class of HPPD inhibitors is represented by pyrazole derivatives (Figure 10). The pyrazoles showed the common structural motif shared by the triketone HPPD inhibitors, that is an α,α-diketo system able to undergo to enolization and to bind an iron ion within the HPPD binding site, as well as an electron-deficient benzoyl moiety with a benzene ring bearing an ortho substituent. Similar to the case for triketones, binding of the pyrazoles to HPPD and inhibition of its enzymatic activity are responsible for bleaching symptoms consequent to pigment destruction.[89] Treatment of photobleached plants with **2** could serve as an antidote to **12**, one of the marketed pyrazole derivatives, thus suggesting that HPPD is the target of this compound and that the inhibitor is displaceable from the HPPD binding site. As already found for other HPPD inhibitors, corn growth is only marginally affected by treatment with **12** and the herbicidal activity is favored by acidic pH values. The main reason for corn selectivity was found by means of metabolic studies. In fact, after a 48 h treatment, the unchanged compound was found to be only 31 and 14 % in foliar and meristematic tissues, while the remaining percentage was

represented by the major metabolite *N*1-desmethyl **12** (about 25- and 50-fold less active in vitro toward HPPD and in vivo in plants, respectively) and additional, minor metabolites.

Intensive studies on pyrazole derivatives allowed the major relationships between their structure and biological activity to be defined (Figure 21). In particular, small alkyl groups are preferred at the N1 of the pyrazole ring, with a methyl group leading to the most active and plant-selective compounds, such as **12** . Moreover, substituents and substitution pattern on the phenyl ring play a pivotal role in determining activity. A halogen (chlorine is the best) or a small alkyl group (a methyl is preferred, while an ethyl and *t*-butyl group is tolerated) at the *ortho*-position of the phenyl ring is a mandatory condition for high activity. An additional electron-withdrawing substituent at the *para*-position (a -SO_2Me is the best for activity) confers further improvement of activity. Active compounds were also found among 1,2,3,4-tetrasubstituted phenyl derivatives. As an example, a *p*-alkoxyphenyl substituent at position 3 of the benzoyl core yielded compounds with activity against weeds and crop selectivity.[28]

10.1. Pyrazole-based hybrid compounds: pyrazole-quinazolones

A scaffold-hopping drug design strategy to find new inhibitors of human HPPD was applied starting from known pyrazole compounds such as **3**, **12**, and **13**. The fact that the quinazolone scaffold was involved in "extensive biological activities" suggested to design hybrid pyrazolo-quinazolones as putative novel HPPD inhibitors (Figure 22).[90] Despite the seemingly weak rationale of this study, many of the new compounds showed a two-digit nanomolar inhibitory activity toward a human recombinant HPPD, comparable to or better than that found for **14** (K_i = 37 nM). Molecular docking simulations were performed with GOLD to check whether the hybrid compounds could be able to interact with the HPPD binding site. An analysis of the resulting theoretical complexes suggested the introduction of a substituted phenyl ring at the N3 of the

quinazolone ring with the aim of improving the contacts between the ligand and the enzyme. Among compounds of the first series, although populated by *ortho*-halo (F and Cl) derivatives with activity of about 80 nM, many showed activity values higher than 100 nM. Such a reduced activity (compared to **14**) was attributed to steric clashes between the 3-methyl group of the pyrazole ring and the amino acids of the HPPD binding site. On this basis, the additional *des*-methyl derivatives were synthesized, which showed a significant enhancement of their activity. In particular, electron withdrawing small substituents (such as F, Cl, and Br) at the ortho position of the phenyl ring were more profitable than a methyl or methoxy group and showed activity in the range between 15 and 24 nM. A similar trend with comparable activity values was found for the same substituents at the para position. The most active compounds showed a *m*-halogen atom (F, Cl, and Br with a 20, 10, and 14 nM activity, respectively), although electron-donating groups (namely, Me and MeO) maintained a 13 and 34 nM activity, respectively. In general, di-substituted derivatives were less active, with the exception of the 2-Br,4-Me analogue (11 nM) that was one of the most active compounds.

10.2. Pyrazole-based hybrid compounds: pyrazole-benzimidazolones

The same approach was applied to design new pyrazolo-benzimidazolones (Figure 22).[91] Also in this case, several of the studied compounds had IC_{50} values (toward human recombinant HPPD) comparable to or better than that of **14** (68 nM). SAR analysis clearly suggested that position 3 of the pyrazole ring should be left unsubstituted as already found with previous pyrazole-quinazolones,[90] while alkyl chains of variable length are tolerated at the nitrogen atoms of the benzimidazolone moiety. In particular, given a 3-unsubstituted pyrazole scaffold, when a Me, Et, or Pr group was placed at one of the benzimidazolone nitrogen atoms, the most active compounds were built with a Et, Pr, or *i*Pr substituent at the second nitrogen. Among congeneric compounds,

inhibitory activity followed the Et≥Pr>*i*Pr order. Derivatives with bulkier alkyl substituents or aryl moieties underwent a significant drop in activity, up to single-digit micromolar concentrations.

11. Isoxazole derivatives: unexpected HPPD inhibitory activity

Isoxazole derivatives were first discovered within a research project aimed at finding new inhibitors of the hydroxymethylglutaryl coenzyme A reductase. A pyrimidinedione (**47**, Figure 23), whose structure was reminiscent of the already known cyclohexanedione herbicides, showed somewhat activity toward selected weeds.[66] Expectedly, the next step was the introduction of the benzoyl moiety found in **14**, thus leading to a hybrid triketone system (**48**) with significantly enhanced activity. Opening of the dione ring to a non-cyclic bis-benzoyl compound (**49**) gave the opportunity to find the first benzoylisoxazole (**50**) that was in turn optimized to **23**.

The significant HPPD inhibitory activity of isoxazole derivatives was unexpected on the basis of the lack of any diketo (enolizable) moiety in their molecular structure. However, as early as 1891,[92] 3-unsubstituted isoxazoles were known to isomerize to α-cyanocarbonyl derivatives when first dissolved in aqueous alkali (such as NaOH) and then neutralized or acidified, as done during the oxygen consumption assay performed to evaluate the HPPD inhibitory activity of **23** and its precursors. The consequent hypothesis was that the 4-ketoisoxazole compounds could give a cyanodiketone derivative responsible for anti-HPPD activity. In agreement, a change of the assay protocol consisting in using a DMSO solution of the putative HPPD inhibitor instead of the aqueous solution resulted in the loss of activity in the case of isoxazole compounds, while all the compounds which had a pre-existing diketone or triketone moiety in their structure (such as **14**, 4-keto-5-hydroxy-pyrazoles, and cyanodiketones) maintained the same activity previously found

in aqueous solution. These results confirmed that activity of isoxazoles toward HPPD was due to the formation of their metabolic cyanodiketone derivative (such as **24**, Figure 1), *via* isoxazole ring opening that can quickly occur by non-enzymatic hydrolysis both in plants and soils.

An interesting study on the activity of **24** was performed on highly purified HPPD from *Daucus carota* (carrot, Apiaceae).[31] Experimental evidence showed a slow and tight binding of **24** to HPPD independent of the presence of oxygen, and slow dissociation of the complex (2 h as the half-life of the complex), and a K_d = 6 nM. These parameters suggested that **24** is a "nearly irreversible inhibitor". Moreover, **24** competes with the substrate **1**, and was able to bind to HPPD only in the presence of ferrous ions, thus suggesting that this cofactor was of pivotal importance for HPPD/inhibitor complex stabilization, in agreement with that found in X-ray complexes where a keto-enol system of the inhibitor was coordinated by an iron ion. The stoichiometry of the interaction suggested a half-site occupancy of enzyme, such that only one mole of inhibitor was enough to fully inhibit one mole of the dimeric HPPD. The half-site occupancy was also confirmed for **24** toward *Pf*HPPD, where two moles of **24** were required to inhibit a tetrameric form of HPPD. Half-site occupancy was specific to **24**. In fact, HPPD inhibitors belonging to different chemical classes, such as a **15**-like compound, were able to fully inhibit HPPD with a 2:1 stoichiometry (two moles of the inhibitor inhibit a mole of the dimeric HPPD).

The identification and development of heterocyclic inhibitors of HPPD, such as pyrazole and isoxazole compounds, has been recently reviewed.[93]

12. Common minimum pharmacophoric pattern

Early SAR studies on several classes of HPPD inhibitors, including pyrazoles, isoxazoles and the corresponding cyanodiketone metabolites, triketones, as well as 2-benzoylresorcinols (**51**, Figure 24),[75] led to the suggestion that the common minimum structural feature shared by these compounds could be represented by an aryldiketone system. In further detail, considering that the β-diketone system undergoes enolic tautomerization in solution, the 2-benzoylethen-1-ol moiety was finally identified as the essential pharmacophore for a significant inhibition of the HPPD enzymatic activity. Further SAR analysis on simple benzoylethenol derivatives showed that the acidity is an important parameter to be taken into account for an efficient inhibition of HPPD, being pK_a values lower than 6 required for an in vivo potent inhibition at least in plants.

13. Benzoyl-benzothiazines

In the search for HPPD inhibitors, a series of benzothiazine dioxide compounds bearing the usual substituted benzoyl moiety at position 3 and the general pharmacophore previously described, was designed (Figure 25).[94] Among about forty new compounds, the most active entry was **52**, with an *o*-Cl,*p*-SO_2Me substitution pattern on the pendant phenyl ring, reminiscent of **15** and other similar triketones. Unexpectedly, compounds with different substituents at both positions ortho and para (such as the *o*-NO_2,*p*-SO_2Me substitution pattern found in **16** and known to be very profitable for HPPD inhibition) were not tested. HPPD inhibitory activity of **52** (IC_{50} = 480 nM toward recombinant *At*HPPD) was comparable to that of **15** (530 nM) and slightly lower than that of **16** (250 nM). The herbicidal activity profile of **52** was characterized by a complete growth inhibition for most of the weed plants assayed both in pre- and post-emergence experiments. Unfortunately, none of these new compounds were assayed toward human or mammalian HPPD.

14. Additional HPPD inhibitors from natural sources

The ability of **26** to inhibit HPPD enzymatic activity prompted the researchers to search for alternative naturally-occurring compounds with the same mechanism of action. The first report of a natural compound with bleaching properties described usnic acid **53** (Figure 26), a secondary metabolite of the yellow-green lichen *Alectoria sarmentosa*.[95] The (-)-enantiomer of **53** induced a dose-dependent inhibition of carotenoid biosynthesis *via* inhibition of *At*HPPD. This compound was described as an irreversible inhibitor of HPPD, similarly to synthetic triketones, such as **15**. In particular, IC_{50} of **53** was found to be 70 nM, better than that of **15** itself. Activity of **53** toward HPPD was ascribed to its triketone system, known to bind the iron ion and the HPPD binding site.[96] An attempt to find additional HPPD inhibitors from natural sources led to the biological evaluation of more than 30 small molecules belonging to different chemical classes. However, none of the test compounds showed a better activity in comparison to (-)-**53**.[97]

Another study evaluated the HPPD inhibitory activity of ethanol extracts of 91 plants from central Argentina.[98] Pinocembrin (**54**, Figure 26), a flavanone derivative, was found to be a reversible and non-competitive inhibitor of pig liver HPPD with an IC_{50} value of 73 μM. Molecular docking calculations suggested for this compound a binding site within HPPD not overlapping that of other known inhibitors, such as the triketone derivatives. This alternative binding mode, supportive of the non-competitive mechanism of action, was consequent to the presence of the keto-enol moiety within the rigid fused chromenone ring, differently from that found in other HPPD inhibitors that showed a certain structural flexibility.

15. Design of HPP analogues as HPPD inhibitors

In the past, it was hypothesized that the α-carbonyl moiety of **1** could undergo a nucleophilic attack leading to a tetrahedral intermediate. On this basis, derivatives of **1** were designed and synthesized with the α-keto group transformed into the corresponding hydrated form (Figure 27). These compounds lacked the possibility to serve as an HPPD substrate and then could inhibit its enzymatic activity by competition with the natural substrate. To prompt the α-keto group to hydration, a fluorine atom was introduced on the methylene bridge of the β-position. The simple 3-F-3-phenylpyruvic acid **55** was found to exist only in the hydrated form (>99%) in water or deuterated water. This compound, competitive inhibitor of pig liver HPPD with a weak inhibition constant (about 10 μM), was not further profiled.[99]

16. Cation chelators as HPPD inhibitors

Hydroxamic acids **56-58** were the first compounds of this structural class to be found as HPPD inhibitors (Figure 27). They showed a weak inhibitory activity (in the two-digit micromolar range) toward *At*HPPD in the enol-borate assay.[100] Their mechanism of action was not investigated, even if activity was probably due to their known ability to chelate both bivalent (such as ferrous ions) and trivalent cations. Since a clear correlation between phytotoxicity and HPPD inhibition was not found, it was hypothesized that HPPD was only partially involved and that other targets (such as metalloenzymes) were affected.

17. Computational protocols to find new HPPD inhibitors

Following a classical computer-based ligand design, HPPD inhibitors were also used to build and validate both ligand- and target-based virtual screening protocols. The last were in turn applied to both the pharmaceutical and the agrochemical field to allow the identification of compounds with

an improved HPPD inhibitory activity.[101] In an effort to find new compounds active toward plants, given that the 3D coordinates of the full length HPPD from plants were not available, a homology model of the *At*HPPD was built starting from the corresponding structure of *S. avermitilis*. The modeled structure was then used to perform docking calculations and the resulting structural features were then codified into a 3D pharmacophoric model, manually adjusted to account for the interactions between the ligand/inhibitor and iron ions. The pharmacophore was submitted to a poor validation step, by correlating the experimental IC_{50} of several HPPD inhibitors with their calculated fit values (expressed as the ability of each compound to map the pharmacophoric portions of the model).[102] Unusually, neither the homology model of *At*HPPD nor the pharmacophore were further used to perform virtual screenings and find new small molecules able to affect HPPD activity.

Following a different approach, a quantitative theoretical model that correlated the inhibitory activity of several phenylquinazolone-pyrazolones already known[90] with their molecular descriptors, such as HOMO and LUMO orbitals, was generated by linear multiple regression analysis.[103] Unexpectedly, the methylated pyrazolone analogues that were reported in the same paper and that could allow to enlarge the range of K_i values, were not taken into account to generate the model. The resulting best equation suggested the optimal groups to be used as substituents at various positions of the phenylquinazolone-pyrazolone scaffold. Also in this case, suggestions coming from the quantitative models were not further applied for the identification of new HPPD inhibitors, thus not allowing for a full validation of the same models.

A docking-based computational approach aimed at further optimizing HPPD inhibitors suggested that different interactions with the HPPD binding site (not clearly detectable at a visual inspection of the corresponding X-ray crystal structure 1SQI and 1TFZ, respectively) and the consequently

different docking energies could be responsible for the high selectivity of **4** for plant enzyme and for the non-selective activitiy of **3** toward both rat and plant HPPD.[104] Based on these calculations, two original compounds were proposed. In detail, **4** was transformed into the corresponding *N*1-2,4-dihydroxy-benzoyl analogue, predicted to be more selective toward plant HPPD in comparison to its parent compound. On the other hand, an analogue of **3** with a 2,4-dichlorophenyl substituent instead of the -SO_2Me group was hypothesized to have a better affinity for both plant and rat enzymes. Again, this hypothesis was not fully validated as the new compounds were neither synthesized nor tested.

18. HPPD inhibitors in therapeutic interventions: the case of compound 14

Dysregulation of enzymes involved in the Phe-Tyr catabolic pathway is linked to various human diseases. As an example, deficiency of TAT enzyme caused by mutations in *TAT* gene is found in type II tyrosinemia (Richner-Hanhart syndrome), an autosomal recessive inherited disease.[105] The disease is characterized by hypertyrosinemia with oculocutaneous manifestations and, in some cases, mental retardation. Management of the disease includes dietary restriction of Phe and Tyr. Such a controlled diet allows lowering of plasma Tyr levels and rapid resolution of the oculocutaneous manifestations, though the effects on CNS are less clear.

Moreover, deficiency of HPPD caused by mutations in *HPD* gene is responsible for type III tyrosinemia, where the accumulation of **1** might eventually lead to elevated blood Tyr levels due to reversibility of the TAT-catalyzed reaction. The disease is characterized by mild hypertyrosinemia and variable clinical pictures.

Increased blood Tyr amounts and consequent ocular manifestations are found also in T1T and in alkaptonuria patients treated with **14** (see below). Both T1T and alkaptonuria are metabolic

diseases arising from defects downstream of production of **2** in the Tyr degradation pathway. In particular, mutations affecting the activity of FAH cause T1T, a fatal disease with autosomal recessive inheritance.[106] The inability of FAH to finalize the Tyr metabolic pathway leads to the non-enzymatic reduction of both fumarylacetoacetate and its precursor maleylacetoacetate into succinylacetoacetate, which is in turn decarboxylated to give succinylacetone (Figure 28). The last two compounds accumulate in high amounts in the liver and kidneys, affecting cellular morphology and organ architecture because of altered redox equilibria. Hepatotoxicity, hepatic lesions, failure and cirrhosis, as well as primary liver cancer can occurr. It was also hypothesized that the mutagenic effects of fumarylacetoacetate may contribute to the initiation steps that lead to cancer.[107]

Alkaptonuria is consequent to gene mutations that cause the inability of HGD to catabolize **2**, which is then accumulated. Evidence suggests tha **2** can undergo oxidation into the corresponding benzoquinone derivative (benzoquinone acetate, BQA) whose polymerization yields a black pigment found in connective tissues and urine of affected individuals (Figure 9). Deposition of such a black pigment (a phenomenon known as ochronosis) causes dramatic degeneration of connective tissues in affected organs, mainly joints[108-111] and cardiac valves,[112-113] although any tissue expressing HGD may be involved.[114-115]

Blocking the production of succinylacetoacetate/succinylacetone and **2** could represent useful therapeutic interventions to treat T1T and alkaptonuria, respectively. As triketone compounds such as **14** were known inhibitors of HPPD in plants, hypotheses were made on their possible use in these human diseases. In T1T, treatment with **14** led to a significant relief of anemia induced by succinylacetone-dependent inhibition of heme synthesis. The application of **14** as a therapeutic

agent for T1T also stimulated work on fumarylacetoacetate and its involvement in mutagenic changes hypothetically responsible for liver tumors in infancy and childhood.

Moreover, **14** recently entered clinical trials to evaluate its efficacy and safety in alkaptonuria as well.[116] In these cases, as expected, one major side effects found for the use of **14** was a combined effect of accumulation of **1** and its re-conversion in Tyr, which was responsible for corneal opacity and ocular lesions very similar to those found in type II tyrosinemia.

A role for **14** was hypothesized also for hawkinsinuria, a disease characterized by the presence of the unusual cyclic amino acid hawkinsin in urine. Erroneously, it was first hypothesized that hawkinsinuria could be caused by A33T substitution in HPPD, which was later demonstrated to be a polymorphic form of HPPD without pathological consequences. Conversely, the mutation responsible for hawkinsinuria in humans involves a N241S substitution, leading to enzyme activity loss and production of hawkinsin through a quinolacetic acid intermediate (Figure 7). From a mechanistic point of view, the quinolacetic acid undergoes first a Michael addition involving cysteine amino acids, then keto-enol tautomerization and reduction of ene system ensue to yield hawkinsin. Fortunately, hawkinsinuria is a temporary disease whose symptoms, described as failure or inability to thrive, disappear after the first 1-2 years of life. Considering that the N241S variant of HPPD is susceptible to the inhibitory activity of **14** probably because "the mutation does not change the binding mechanism significantly",[39] such a compound could be used in the very first years of life of infants suffering from hawkinsinuria.

19. Pharmacokinetics and Toxicity of HPPD inhibitors in mammals

Early studies on the toxicity of triketones were focused on experimental animals, such as rats and mice. In particular, the mechanism of action established for **16** on mammals was based on a

competitive and reversible inhibiton of HPPD, with consequent accumulation of its substrate **1**. Since the metabolic step catalyzed by TAT is reversible, significant accumulation of Tyr was evident as well. TAT enzyme activity is also responsible for species- and genre-dependent differencies in Tyr accumulation. For instance, male rats treated with HPPD inhibitors can accumulate Tyr up to about 3 mM, while two-fold reduced levels can be found in female rats. Differently, the highest observed Tyr level in mice was around 0.8 mM. The impressive increase of Tyr levels in rats is responsible for a wide panel of adverse effects not found in mice.[117] The different toxicity in rats and mice, combined with the reduced activity of TAT in rats, suggests that adverse effects observed after triketone administration are not related to intrinsic toxicity of these compounds, but they are rather consequence of excess Tyr in blood. Further support to this hypothesis is provided by the fact that blood Tyr below 0.5 mM is not associated to adverse effects. Moreover, when administered at comparable doses in T1T patients, **16** is associated to lower Tyr levels respecting to **14**: this is related to a shorter half-life of **16** (≈ 1 hour) compared to **14** (≈ 53 hours). Thus, both drug half-life and TAT activity can be considered pivotal elements contributing to tyrosinaemia and related side-effects in humans.[117]

Hypertyrosinemia induced by **14** is not straightforwardly related to corneal injuries, as differencies in TAT enzymatic activity play a significant role in modulating **14**-induced ocular toxicity. Administration of **14** to mice caused quick suppression of HPPD activity and marked increase of Tyr levels in plasma and aqueous humor. However, any ocular toxicity and corneal injury was found, differently to what found in rats treated with **14** and in rats fed with Tyr-enriched diet.[118] Furthermore, hypertyrosinemia induced corneal lesions in dogs but not in rabbits.[119]

When **67** was tested in rats to assess its effects on hepatic enzymes involved in Tyr pathway, a quasi-quantitative inhibition of HPPD was found (from 91 to 96% in comparison to control, depending on the dose of **15**) together with a significant decrease (29-46%) in HGD activity and a significant increase (43-175%) in TAT activity. Such an effect of **15** in TAT activity differed from what observed with **14**, which indirectly inhibited TAT through HPPD repression and accumulation of **1**. The same corneal lesions associated to **14** and Tyr-enriched diet were described also with **15**. Partial opacity was observed at week 2 after a 50 and 100 mg/kg/day dosage.[79] Complete opacity was reached at the end of the treatment (90 days), that regressed one week after discontinuation of administration. A chronic keratitis was also observed, with the epithelium and the stroma that underwent significant structural modifications. Rats treated with **15** showed markedly increased Tyr levels both in plasma (up to 15-fold) and in the eye (up to 5-fold), with ocular Tyr level higher than what found in plasma. Thus the observed corneal lesions could be due to the formation of crystals within cells and/or alteration of redox equilibria upon formation of tyrosyl radicals, although the presence of other factors coud not be ruled out. Different results were reported in humans, where Tyr levels did not increase significantly after administration of **15**, even in cases of poisoning after voluntary ingestion of a commercial herbicide containing **15**.[120-121] Only transient symptoms were described (such as high plasma concentrations of **15**, mild hypertyrosinemia, and renal failure) that did not evolve in permanent damages. Tyrosinemia was however below the threshold recommended by FDA for treatment with **14**.

Administration of **14** and **16** to healthy male volunteers showed that the two compounds had very different pharmacokinetic and pharmacodynamics profiles, although sharing common portions in their chemical structures. Both were rapidly absorbed and acted as HPPD inhibitors, although

with different magnitude and duration.[122] In particular, **16** (at the dose of 4 mg/kg body weight) showed a plasma half-life of about 1 h and was rapidly eliminated unchanged in urine. It induced a minimal increase of plasma Tyr from 0.036-0.105 mM (with a controlled diet) to about 0.3 mM within 2 days. Differently, **14** induced a rapid inhibition of the HPPD activity (with a rate constant of $9.9 \cdot 10^{-5}$ $s^{-1} \cdot nM^{-1}$ in rats) followed by a slow complex dissociation (in vitro half-life of 63 and 53 h in rats and humans, respectively) with consequent recovery of enzyme activity. This means that **14** is not an irreversible HPPD inhibitor but is characterized by a long residence time in comparison to other triketones; it only competes with the natural substrate for the same binding site. At the dose of 1 mg/kg body weight, **14** showed a persistent activity toward HPPD in human mainly due to its long half-life. A significant increase of plasma Tyr levels was found, from 0.076-0.136 mM (uncontrolled diet) to about 1.1 mM within 120 hours. Background levels of plasma Tyr were restored 2 months after dosing.

The different pharmacological profiles of **16** and **14** in terms of magnitude, duration of activity toward HPPD and influence on plasma Tyr levels allowed **14** to be used as a drug and **16** as an herbicide. In fact, **14** is currently adopted to treat T1T and is now in advanced clinical trials for alkaptonuria,[123-124] two diseases that require a persistent suppression of HPPD activity for their treatment. On the other hand, **16**, considered as a safe herbicide also in case of systemic exposure during industrial preparation or application in agriculture because of its transient activity toward human and mammalian HPPD, is used to control weeds in maize crop.

Compound **17**, another member of the triketone class, has been classified as a low risk compound for most of the terrestrial and aquatic animals and for terrestrial non-target plants, while the most sensitive species are aquatic plants.[125] Compound **17** is rapidly absorbed and completely excreted after 96 h, without significant accumulation, although associated, as expected, to corneal lesions,

as well as liver and kidney toxicity in rats. Risks for consumers or after occupational exposure are significantly below the acceptable cutoff.[125] Although literature reports did not describe **17** as a genotoxic compound, a recent study on human hepatocellular carcinoma cell line HepG2 suggested caution to be taken when using it. In fact, cytogenetic effects were highlighted in HepG2 cells, even if a low cytotoxicity and negligible DNA damage were measured at residential and operator exposure levels (2 and 1.2 mg/mL, respectively).[126]

Metabolic studies on triketones showed that the main route of metabolism was an hydroxylation at position 4 of the cyclohexyl ring or, alternatively, the same reaction at position 6 (chemically equivalent) in the presence of substituents at position 4. As an example, 4-hydroxyl derivative of **15** was found as the major metabolite of the parent compound in rat urine. In a similar way, a stepwise hydroxylation at the cyclohexyl ring also occurred for **17**. Accordingly, mono and dihydroxylated metabolites of **17** were found both in plants, animals, and soil. These findings allowed to account for different herbicidal activity of compounds sharing the same HPPD binding affinity. In particular, better herbicides were the compounds with the metabolic labile positions occupied by substituents. Despite their higher metabolic stability and herbicidal potency, these molecules were not prioritized because of their lack of selectivity toward maize and increased soil persistence, which can negatively affect crop rotation, particularly soybean crops.[54] However, further studies on the same class of compounds led to the identification of **19** and **21** that bear an ethyl bridge linking positions 4 and 6 of the cyclohexyl ring, thus preventing metabolic degradation. They are currently under study for their weed inhibitory activity in rice and corn crops.

Pyrazole derivatives undergo dealkylation at the *N*1 pyrazole ring. In fact, the major metabolite of **12** is an *N*1-demethylated derivative that shows a significantly lower activity toward *At*HPPD in comparison to the parent compound (600 vs 23 nM).[89]

On the other hand, as a general trend for environmental fate, soil metabolites of triketones and isoxazoles are represented by the corresponding substituted benzoic acid. As an example, **15** is found in soil as the 2-chloro-4-methylsulfonyl-benzoic acid metabolite, which is classified as a low risk compound for environmental toxicity. In a similar way, the 2-nitro-4-methylsulfonyl-benzoic acid is found as a metabolite of **16**, in addition to the corresponding amino derivative generated by reduction of the nitro group. Recently, bacterial strains were isolated from soil and cloud water that were able to completely and rapidly degrade **15** and **16**,[127-128] chemical entities classified as toxicologically dangerous for the environment.

A recent survey on hygienic classification, sensitivity of experimental animals and toxicity on them, has been reported for the most important triketones, isoxazoles, and pyrazoles used as active ingredients of currently available herbicides.[129] More complete information on such compounds, including environmental fate (i.e., soil absorption, mobility, and degradation, as well as soil, animal, and plant metabolites), ecotoxicology (LC_{50} and LD_{50} in animals, and amount of compounds found in plants), and human health issues could be find at the Pesticide Properties Database (PPDB).[130]

20. Triketones inhibitors of HPPD also showed additional biological activities

Both naturally occurring triketones and their synthetic derivatives also showed a wide spectrum of activities toward microorganisms. Compound **14** and other HPPD inhibitors have been patented as tools for the treatment of microbial infections, on the basis of their ability to reduce

the production of pigments in microorganisms. Reduced amounts of pigments are known to increase the susceptibility of microorganisms to drugs. In fact, microorganisms become less resistant to macrophage attack and phagolysosomal fusion when they have a disregulated production of pigments.[131] In other examples, essential oils from *L. scoparium* (in particular, the so called manuka oil of the Australian tradition)[70] and from *Melaleuca alternifolia* (Myrtaceae, the so called tea tree oil)[132] showed antimicrobial activity mainly due to their triketone complex that contained a significant amount of **26** and its analogues. However, only gram-positive bacteria are susceptible to natural triketones[70,132] and their synthetic derivatives.[133] Manuka oil was also found to inhibit the growth of *Herpes simplex* virus type 1 and 2, being **26** and flavesone (two components of the triketone complex) the active compounds.[134]

Recently, a pivotal study on the application of HPPD inhibitors as anti-plasmodial agents has been reported.[135] A structurally heterogeneous class of β-triketones bearing a syncarpic acid moiety (referred to as watsonianones) were isolated from *Corymbia watsoniana* (Mirtaceae) and assayed as inhibitors of *Plasmodium falciparum*. The most active compound (namely, watsonianone B, **59**, Figure 29) showed a sub-micromolar activity toward both chloroquine-sensitive and -resistant strains of the parasites (IC_{50} = 0.4 and 0.3 μM, respectively) and represented an innovative chemotype for inhibition of *P. falciparum*.

A subsequent study on human parasites led to the discovery that blood-feeding arthropods are selectivity killed by HPPD inhibitors.[136] Enzymes involved in Tyr degradation (TAT and HPPD) are overexpressed after a blood meal and their inhibition caused insect death. As an example, **16** is able to selectively kill blood-feeding arthropods by Tyr accumulation. More interestingly, since oogenesis was incomplete before death, HPPD inhibitors can also block insect reproduction. Insects are also killed when they feed on mice treated with **14** (1 mg/kg body weight). Non-

hematophagous insects are not affected by HPPD inhibitors. These results are very important because they lay the foundations for new selective insecticides, in principle more active toward arthropods that are increasingly resistant to the currently available neurotoxic agents.

HPPD inhibitors have been also patented for their possible application in the treatment of depression,[137] restless leg syndrome and related sleep disorders,[138] as well as in people suffering from Parkinson's diseases (PD).[139] In these cases, inhibition of HPPD could guarantee elevated levels of plasma Tyr that are expected to increase brain dopamine, being Tyr the precursor of dopamine itself. Studies on PD were discontinued after a phase 2 clinical trial that "did not show a significant improvement in measures of PD motor function when compared to placebo".[140] For the remaining studies, no results have been disclosed yet.

Compound **14** is also currently under phase 1/2 clinical trials for oculocutaneous albinism, type 1B,[141] being able to ameliorate skin and eye pigmentation in a mouse model of the disease.[142-143] In fact, by increasing plasma Tyr levels to millimolar concentrations (about 0.7-0.8 mM) after administration of **14** in clinical isolates (from patients with oculocutaneous albinism, type 1B) and albino mouse models (4 mg/kg every other day) with a residual tyrosinase activity, tyrosinase is stabilized and its activity enhanced. As a consequence, an increase of melanin levels in intracellular melanosomes is observed, together with increased pigmentation of both iris and new hair in mice. The enhanced pigmentation has been hypothesized to ameliorate the visual function in people suffering from albinism type 1B, although a robust correlation between pigment deposition and visual function was not demonstrated even in mice.[142] Importantly, on the basis of the fact that Tyr could serve as a substrate chaperone for correcting the misfolded tyrosinase in cases of oculocutaneous albinism type 2, studies for repositioning of **14** as a drug could be further extended to this human disease.[144]

21. Conclusion and future directions

This review describes interesting interconnections between agrochemicals and drug-like compounds, the most striking example being studies on plant HPPD inhibitors used in the agrochemical context as bleaching herbicides that led to the repositioning of **14** as a drug for human diseases. In particular, **14** is currently used to interfere with Tyr metabolic pathway to treat T1T, an inherited and fatal disease. Moreover, a possible application of **14** as a drug for the treatment of alkaptonuria is under evaluation in clinical trials. Finally, treatment with **14** could be also beneficial for hawkinsinuria, a transient disease caused by HPPD mutants that are however sensitive to **14**. These considerations highlight the importance of drug repositioning approach in finding new uses for well-known drugs. For **14**, a reasoned (not serendipitous) repositioning was made possible by an in depth analysis of the mechanism of action of triketone herbicides, as well as of their side effects in experimental animals during toxicity assays. Moreover, repositioning of **14** is unique for the fact that, by interfering with the Tyr metabolic pathway, it is possible to treat T1T, alkaptonuria, and (possibly) hawkinsinuria.

Another interesting example falling within the same experimental context and rational design is the serendipitous discovery of the allelopathic properties of triketones from *Callistemon* sp. plants. This was the starting point for design, synthesis, and biological evaluation of a significant number of new chemical entities belonging to different structural classes. Additional efforts for the identification of novel small molecules able to interfere with HPPD enzymatic activity, still ongoing, are summarized in this review.

However, design of an effective and safe HPPD inhibitor to be used as a drug is a challenging task to be issued. Many of the currently available HPPD inhibitors, such as the drug **14**, are

characterized by a rapid inactivation of the enzyme and a long residence time. This means that the HPPD-inhibitor complex is formed very quickly, but it dissociates very slowly (quasi-irreversible inhibition). As a result of the rapid and persistent HPPD inactivation, an unbalanced ratio between suppressed production of **2** and high Tyr accumulation led to important side effects. In this context, a fine modulation of HPPD activity is required by means of compounds with reduced residence time. By this way, a partial reactivation of HPPD will guarantee a limited production of **2** and avoid too high levels of tyrosinemia. In particular, a rapid complex dissociation will result in the desired pharmacology, while prolonged residence time will cause unwanted effects.

On the other hand, HPPD inhibitors with different pharmacokinetics and pharmakodynamics properties could be selected as safe herbicides. As an example, **16** is characterized by a specific plant selectivity profile that renders this compound an effective herbicide for maize protection. At the same time, on the basis of its short plasma and HPPD-complex half-life in mammals, **16** is considered as a safe herbicide. This means that herbicide selection requires a careful evaluation of toxicity toward the environment and end-user, in addition to have a wide activity for weed control, low application rates, and crop selectivity.

Author information

Corresponding Author

*Phone: +39 0577 234330. E-mail: fabrizio.manetti@unisi.it

Notes

The authors declare no competing financial interest.

Biographies

Annalisa Santucci is a Full Professor of Biochemistry at the Department of Biotechnology, Chemistry and Pharmacy, of Siena University. Author of 200 papers on international peer-reviewed journals, and inventor of 7 patents. Recently, AS developed unique expertise in alkaptonuria physiopathological molecular mechanisms; her group developed a series of in vitro and ex vivo alkaptonuria human models; she discovered secondary amyloidosis and links between inflammation and oxidative stress in alkaptonuria. Member of the Advisory Board of FindAKUre international network. Founder, Vice-President and President of the Scientific Committee of aimAKU (Associazione Italiana Malati di Alcaptonuria). Organizer of six editions of AKU International Workshop (2009-2013) and 1st Italian Meeting on AKU (2015). Several funds obtained for AKU research, including: FP7-HEALTH-2012-INNOVATION-1 - Clinical Development of Nitisinone for Alkaptonuria.

Giulia Bernardini is a Research Assistant in Biochemistry at the Department of Biotechnology, Chemistry and Pharmacy, of Siena University. GB's scientific background is primarily in

biochemistry, with a focus on post-genomics and differential protein expression analysis. Her research interests embrace a wide array of scientific topics ranging from proteomics and immunoproteomics of pathogen microorganisms, to proteomics and immunoproteomics of human samples with regard to different pathologies in particular bone metabolic and osteoarticular diseases. Her research is mainly focused in elucidating the molecular basis of diseases such as osteosarcoma and alkaptonuria, and developing novel therapeutic approaches. Author of 60 papers on international peer-reviewed scientific journals, and inventor of 2 patents.

Daniela Braconi is a Research Assistant in Biochemistry at the Department of Biotechnology, Chemistry and Pharmacy (Siena University). Her scientific background is primarily in biochemistry, with several proteomic and immunoproteomic studies related to microorganisms and human diseases, paying particular attention to oxidative post-translational modifications of proteins. In the last years, she focused on the elucidation of molecular mechanisms underlying the rare disease alkaptonuria. She is author of 48 papers in international peer-reviewed scientific journals.

Elena Petricci is Researcher of Organic Chemistry at the Department of Biotechnology, Chemistry, and Pharmacy of the University of Siena, Italy. Her research activity is focused on the application of innovative techniques and methodologies for the synthesis of small molecules within drug design and development research projects.

Fabrizio Manetti, Ph.D., is Associate Professor of Medicinal Chemistry at the Department of Biotechnology, Chemistry, and Pharmacy of the University of Siena, Italy. He is co-founder of

Lead Discovery Siena, a spinoff operating in the field of drug design and lead optimization. His research activity is focused on the application of ligand- and structure-based drug design approaches to find biologically active small molecules.

Abbreviations used

HPPD, 4-hydroxyphenylpyruvate dioxygenase; *Pf*HPPD, *Pseudomonas fluorescens* HPPD; *Zm*HPPD, *Zea mais* HPPD; *At*HPPD, *Arabidopsis thaliana* HPPD; *Sa*HPPD, *Streptomyces avermitilis* HPPD; *Rn*HPPD, *Rattus norvegicus* HPPD; NTBC, 2-[2-nitro-4-(trifluoromethyl)benzoyl]cyclohexane-1,3-dione, nitisinone; PAH, phenylalanine-4-hydroxylase; FAH, fumarylacetoacetate hydrolase; HGD, homogentisate dioxygenase; HGA, homogentisic acid; TAT, tyrosine aminotransferase; HPP, 4-hydroxyphenylpyruvate; MAAI, maleylacetoacetate isomerase; UniProtKB, UniProt Knowledgebase database; PIR, Protein Information Resource; MNPBQ, 2-methyl-6-nonaprenyl-1,4-benzoquinone; MPBQ, 2-methyl-6-phytyl-1,4-benzoquinone; DMPBQ, 2,3-dimethyl-6-phytyl-1,4-benzoquinone; DKN, diketonitrile of isoxaflutole; PPDB, Pesticide Properties Database; TH, tyrosine hydroxylase, Tyr, tyrosine; Phe, phenylalanine; T1T, type I tyrosinemia.

References

1. Lindstedt, S.; Holme, E.; Lock, E. A.; Hjalmarson, O.; Strandvik, B. Treatment of hereditary tyrosinaemia type I by inhibition of 4-hydroxyphenylpyruvate dioxygenase. *Lancet* **1992**, *340*, 813-817.

2. Ashburn, T. T.; Thor, K. B. Drug repositioning: identifying and developing new uses for existing drugs. *Nat. Rev. Drug Discov.* **2004**, *3*, 673-683.

3. Langedijk, J.; Mantel-Teeuwisse, A. K.; Slijkerman, D. S.; Schutjens, M. D. B. Drug repositioning and repurposing: terminology and definitions in literature. *Drug Discov. Today* **2015**, *20*, 1027-1034.

4. Nosengo, N. New tricks for old drugs. *Nature* **2016**, *534*, 314-316.

5. Lekka, E.; Deftereos, S. N.; Persidis, A.; Persidis, A.; Andronis, C. Literature analysis for systematic drug repurposing: a case study from Biovista. *Drug Discov. Today Ther. Strat.* **2011**, *8*, 103-108.

6. Iwata, H.; Sawada, R.; Mizutani, S.; Yamanishi, Y. Systematic drug repositioning for a wide range of diseases with integrative analyses of phenotypic and molecular data. *J. Chem. Inf. Model.* **2015**, *55*, 446-459.

7. Calder, A. N.; Androphy, E. J.; Hodgetts, K. J. Small molecules in development for the treatment of spinal muscular atrophy. *J. Med. Chem.* **2016**, *59*, 10067-10083.

8. Bhinder, B.; Djaballah, H. Drug discovery and repurposing at Memorial Sloan Kettering Cancer Center: chemical biology drives translational medicine. *ACS Chem. Biol.* **2014**, *9*, 1394-1397.

9. National center for advancing translational sciences. https://ncats.nih.gov/preclinical/repurpose, accessed August 18, 2016.

10. Naylor, S.; Schonfeld, J. M. Therapeutic drug repurposing, repositioning and rescue. Part I: overview. *Drug Discov. World* **2015**, *winter 2014/15*, 49-62.

11. Drug Repurposing, Rescue, and Repositioning. http://www.liebertpub.com/overview/drug-repurposing-rescue-brand-repositioning/627, accessed August 18, 2016.

12. Drug repositioning, repurposing, and rescue conference. http://www.drugrepositioningconference.com/index, accessed August 18, 2016.

13. Khedr, M. A.; Shehata, T. M.; Mohamed, M. E. Repositioning of 2,4-dichlorophenoxy acetic acid as a potential anti-inflammatory agent: *in silico* and pharmaceutical formulation study. *Eur. J. Pharm. Sci.* **2014**, *65*, 130-138.

14. Lock, E. A.; Ellis, M. K.; Gaskin, P.; Robinson, M.; Auton, T. R.; Provan, W. M.; Smith, L. L.; Prisbylla, M. P.; Mutter, L. C.; Lee, D. L. From toxicological problem to therapeutic use: the discovery of the mode of action of 2-(2-nitro-4-trifluoromethylbenzoyl)-1,3-cyclohexanedione (NTBC), its toxicology and development as a drug. *J. Inher. Metab. Dis.* **1998**, *21*, 498-506.

15. Holme, E.; Lindstedt, S. Tyrosinaemia type I and NTBC 2-(2-nitro-4-trifluoromethylbenzoyl)-1,3-cyclohexanedione. *J. Inher. Metab. Dis.* **1998**, *21*, 507-517.

16. Braconi, D.; Millucci, L.; Bernardini, G.; Santucci, A. Oxidative stress and mechanisms of ochronosis in alkaptonuria. *Free Radic. Biol. Med.* **2015**, *88*, 70-80.

17. Moran, G. R. 4-Hydroxyphenylpyruvate dioxygenase. *Arch. Biochem. Biophys.* **2005**, *433*, 117-128.

18. Moran, G. R. 4-Hydroxyphenylpyruvate dioxygenase and hydroxymandelate synthase: exemplars of the α-keto acid dependent oxygenases. *Arch. Biochem. Biophys.* **2014**, *544*, 58-68.

19. Human 4-hydroxyphenylpyruvate dioxygenase, http://www.uniprot.org/uniprot/P32754, accessed August 5, 2016.

20. The Universal Protein Resource (UniProt), www.uniprot.org, accessed December 5, 2016.

21. Huang, C.; Liu, H.; Shen, C.; Chen, Y.; Lee, S.; Lloyd, M.; Lee, H. The different catalytic roles of the metal-binding ligands in human 4-hydroxyphenylpyruvate dioxygenase. *Biochem. J.* **2016**, *473*, 1179-1189.

22. Protein Information Resource, pir.georgetown.edu/pirwww/search/multialn.shtml, accessed December 5, 2016.

23. Yang, C.; Pflugrath, J. W.; Camper, D. L.; Foster, M. L.; Pernich, D. J.; Walsh, T. A. Structural basis for herbicidal inhibitor selectivity revealed by comparison of crystal structures of plant and mammalian 4-hydroxyphenylpyruvate dioxygenases. *Biochemistry* **2004**, *43*, 10414-10423.

24. Fritze, I. M.; Linden, L.; Freigang, J.; Auerbach, G.; Huber, R.; Steinbacher, S. The crystal structures of *Zea mays* and *Arabidopsis* 4-hydroxyphenylpyruvate dioxygenase. *Plant Physiol.* **2004**, *134*, 1388-1400.

25. Brownlee, J.; Johnson-Winters, K.; Harrison, D. H. T.; Moran, G. R. Structure of the ferrous form of (4-hydroxyphenyl)pyruvate dioxygenase from *Streptomyces avermitilis* in complex with the therapeutic herbicide, NTBC. *Biochemistry* **2004**, *43*, 6370-6377.

26. Serre, L.; Sailland, A.; Sy, D.; Boudec, P.; Rolland, A.; Pebay-Peyroula, E.; Cohen-Addad, C. Crystal structure of *Pseudomonas fluorescens* 4-hydroxyphenylpyruvate dioxygenase: an enzyme involved in the tyrosine degradation pathway. *Structure* **1999**, *7*, 977-988.

27. Berman, H. M.; Westbrook, J.; Feng, Z.; Gilliland, G.; Bhat, T. N.; Weissig, H.; Shindyalov, I. N.; Bourne, P. E. The Protein Data Bank. *Nucleic Acids Res.* **2000**, *28*, 235-242; www.rcsb.org.

28. Siddal, T. L.; Ouse, D. G.; Benko, Z. L.; Garvin, G. M.; Jackson, J. L.; McQuiston, J. M.; Ricks, MJ.; Thibault, T. D.; Turner, J. A.; VanHeertum, J. C.; Weimer, M. R. Synthesis and herbicidal activity of phenyl-susbtituted benzoylpyrazoles. *Pest Manag. Sci.* **2002**, *58*, 1175-1186.

29. Lin, J.; Sheih, Y.; Chang, T.; Chang, N.; Chang, C.; Shen, C.; Lee, H. The interactions in the carboxy terminus of human hydroxyphenylpyruvate dioxygenase are critical to mediate the conformation of the final helix and the tail to shield the active site for catalysis. *PloS ONE* **2013**, *8*, e69733.

30. Kavana, M.; Moran, G. R. Interaction of (4-hydroxyphenyl)pyruvate dioxygenase with the specific inhibitor 2-[2-nitro-4-(trifluoromethyl)benzoyl]-1,3-cyclohexanedione. *Biochemistry* **2003**, *42*, 10238-10245.

31. Garcia, I.; Job, D.; Matringe, M. Inhibition of *p*-hydroxyphenylpyruvate dioxygenase by the diketonitrile of isoxaflutole: a case of half-site reactivity. *Biochemistry* **2000**, *39*, 7501-7507.

32. Discovery Studio 3.0 Visualizer, formerly distributed by Accelrys Software, Inc., now Dassault Systèmes Biovia, http://accelrys.com/products/collaborative-science/biovia-discovery-studio/visualization.html, accessed August 22, 2016.

33. Kaafarani, B. R.; Wex, B.; Oliver, A. G.; Krause Bauerc, J. A.; Neckersa, D. C. π-π-Stacking and nitro-π-stacking interactions of 1-(4-nitrophenyl)-4-phenyl-2,4-bis(phenylethynyl)butadiene. *Acta Cryst. Sect. E* **2003**, *E59*, o227-o229.

34. Borowski, T.; Bassan, A.; Siegbahn, P. E. M. 4-Hydroxyphenylpyruvate dioxygenase: a hybrid density functional study of the catalytic reaction mechanism. *Biochemistry* **2004**, *43*, 12331-12342.

35. Wojcik, A.; Broclawik, E.; Siegbahn, P. E. M.; Lundberg, M.; Moran, G.; Borowski, T. Role of substrate positioning in the catalytic reaction of 4-hydroxyphenylpyruvate dioxygenase – a QM/MM study. *J. Am. Chem. Soc.* **2014**, *136*, 14472-14485.

36. Molchanov, S.; Gryff-Keller, A. Inhibition of 4-hydroxyphenylpyruvate dioxygenase by 2-[2-nitro-4-(trifluoromethyl)benzoyl]1,3-cyclohexanedione. *Acta Biochim. Pol.* **2009**, *56*, 447-454.

37. Raspail, C.; Graindorge, M.; Moreau, Y.; Crouzy, S.; Lefebvre, B.; Robin, A. Y.; Dumas, R.; Matringe, M. 4-Hydroxyphenylpyruvate dioxygenase catalysis. Identification of catalytic residues and production of a hydroxylated intermediate shared with a structurally unrelated enzyme. *J. Biol. Chem.* **2011**, *286*, 26061-26070.

38. Gunsior, M.; Ravel, J.; Challis, G. L.; Townsend, C. A. Engineering *p*-hydroxyphenylpyruvate dioxygenase to a *p*-hydroxymandelate synthase and evidence for the proposed benzene oxide intermediate in homogentisate formation. *Biochemistry* **2004**, *43*, 663-674.

39. Brownlee, J. M.; Heinz, B.; Bates, J.; Moran, G. R. Product analysis and inhibition studies of a causative Asn to Ser variant of 4-hydroxyphenylpyruvate dioxygenase suggest a simple route to the treatment of hawkinsinuria. *Biochemistry* **2010**, *49*, 7218-7226.

40. Diebold, A. R.; Brown-Marshall, C. D.; Neidig, M. L.; Brownlee, J. M.; Moran, G. R.; Solomon, E. I. Activation of α-keto acid-dependent dioxygenases: application of an $\{FeNO\}^7/\{FeO_2\}^8$ methodology for characterizing the initial steps of O_2 activation. *J. Am. Chem. Soc.* **2011**, *133*, 18148-18160.

41. Hawkes, T. R. Hydroxyphenylpyruvate dioxygenase (HPPD): the herbicide target. In *Modern Crop Protection Compounds, Second Edition, Chapter 4: Herbicides with bleaching properties*;

Kramer, W., Schirmer, U., Jeschke, P., Witschel, M., Eds.; Wiley-VCH Verlag GmbH & Co. KgaA: Weinheim, Germany, 2012; pp 225-235.

42. Cheng, Z.; Sattler, S.; Maeda, H.; Sakuragi, Y.; Bryant, D. A.; DellaPenna, D. Highly divergent methyltransferases catalyze a conserved reaction in tocopherol and plastoquinone synthesis in cyanobacteria and photosynthetic eukaryotes. *Plant Cell* **2003**, *15*, 2343-2356.

43. Norris, S. R.; Barrette, T. R.; DellaPenna, D. Genetic dissection of carotenoid synthesis in arabidopsis defines plastoquinone as an essential component of phytoene desaturation. *Plant Cell* **1995**, *7*, 2139-2149.

44. Rosa, A.; Tuberoso, C. I. G.; Atzeri, A.; Melis, M. P.; Bifulco, E.; Dessì, M. A. Antioxidant profile of strawberry tree honey and its marker homogentisic acid in several models of oxidative stress. *Food Chem.* **2011**, *129*, 1045-1053.

45. Wang, H.; Qiao, Y.; Chai, B.; Qiu, C.; Chen, X. Identification and molecular characterization of the homogentisate pathway responsible for pyomelanin production, the major melanin constituents in *Aeromonas media* WS. *PLoS ONE* **2015**, *10*, e0120923.

46. Roberts, N. B.; Curtis, S. A.; Milan, A. M.; Ranganath, L. R. The pigment in alkaptonuria relationship to melanin and other coloured substances: a review of metabolism, composition and chemical analysis. *J. Inherit. Metab. Dis.* **2015**, *24*, 51-66.

47. Solano, F. Melanins: skin pigments and much more – types, structural models, biological functions, and formation routes. *New J. Sci.* **2014**, *2014*, 498276.

48. Lindstedt, S.; Rundgren, M. Inhibition of 4-hydroxyphenylpyruvate dioxygenase from *Pseudomonas* sp. strain P.J. 874 by the *enol* tautomer of the substrate. *Biochim. Biophys. Acta* **1982**, *704*, 66-74.

49. Dayan, F. E.; Duke, S. O.; Sauldubois, A.; Singh, N.; McCurdy, C.; Cantrell, C. *p*-Hydroxyphenylpyruvate dioxygenase is a herbicidal target site for β-triketones from *Leptospermum scoparium*. *Phytochemistry* **2007**, *68*, 2004-2014.

50. Ellis, M. K. ; Whitfield, A. C.; Gowans, L. A.; Auton, T. R.; McLean Provan, W.; Lock, E. A.; Smith, L. L. Inhibition of 4-hydroxyphenylpyruvate dioxygenase by 2-(2-nitro-4-trifluoromethylbenzoyl)-cyclohexane-1,3-dione and 2-(2-chloro-4-methanesulfonylbenzoyl)-cyclohexane-1,3-dione. *Toxicol. Appl. Pharmacol.* **1995**, *133*, 12-19.

51. Ellis, M. K.; Whitfield, A. C.; Gowans, L. A.; Auton, T. R.; McLean Provan, W.; Lock, E. A.; Lee, D. L.; Smith, L. L. Characterization of the interaction of 2-[2-nitro-4-(trifluoromethyl)benzoyl]-4,4,6,6-tetramethyl-cyclohexane-1,3,5-trione with rat hepatic 4-hydroxyphenylpyruvate dioxygenase. *Chem. Res. Toxicol.* **1996**, *9*, 24-27.

52. Laschi, M.; Bernardini, G.; Dreassi, E.; Millucci, L.; Geminiani, M.; Braconi, D.; Marzocchi, B.; Botta, M.; Manetti, F.; Santucci, A. Inhibition of *para*-hydroxyphenylpyruvate dioxygenase by analogues of the herbicide nitisinone as a strategy to decrease homogentisic acid levels, the causative agent of alkaptonuria. *ChemMedChem* **2016**, *11*, 674-678.

53. Copeland, R. A. The drug-target residence time model: a 10-year retrospective. *Nat. Rev. Drug Discov.* **2016**, *15*, 87-95.

54. Mitchell, G.; Bartlett, D. W.; Fraser, T. E. M.; Hawkes, T. R.; Holt, D. C.; Townson, J. K.; Wichert, R. A. Mesotrione: a new selective herbicide for use in maize. *Pest Manag. Sci.* **2001**, *57*, 120-128.

55. Siehl, D. L.; Tao, Y.; Albert, H.; Dong, Y.; Heckert, M.; Madrigal, A.; Lincoln-Cabatu, B.; Lu, J.; Fenwick, T.; Bermudez, E.; Sandoval, M.; Horn, C.; Green, J. M.; Hale, T.; Pagano, P.; Clark, J.; Udranszky, I. A.; Rizzo, N.; Bourett, T.; Howard, R. J.; Johnson, D. H.; Vogt, M.;

Akinsola, G.; Castle, L. A. Broad 4-hydroxyphenylpyruvate dioxygenase inhibitor herbicide tolerance in soybean with an optimized enzyme and expression cassette. *Plant Physiol.* **2014**, *166*, 1162-1176.

56. Ahrens, H.; Lange, G.; Muller, T.; Rosinger, C.; Willms, L.; van Almsick, A. 4-Hydroxyphenylpyruvate dioxygenase inhibitors in combination with safeners: solutions for modern and sustainable agriculture. *Angew. Chem. Int. Ed.* **2013**, *52*, 9388-9398.

57. Witschel, M. Design, synthesis and herbicidal activity of new iron chelating motifs for HPPD-inhibitors. *Bioorg. Med. Chem.* **2009**, *17*, 4221-4229.

58. Kraehmer, H.; van Almsick, A.; Beffa, R.; Dietrich, H.; Eckes, P.; Hacker, E.; Hain, R.; Strek, H. J.; Stuebler, H.; Willms, L. Herbicides as weed control agents: state of the art: II. Recent achievements. *Plant Physiol.* **2014**, *166*, 1132-1148.

59. U.S. environmental protection agency, office of pesticide programs, registration division, https://www3.epa.gov/pesticides/chem_search/ppls/000100-01467-20150424.pdf, accessed December 2, 2016.

60. Jeanmart, S.; Edmunds, A. J. F.; Lamberth, C.; Pouliot, M. Synthetic approaches to the 2010-2014 new agrochemicals. *Bioorg. Med. Chem.* **2016**, *24*, 317-341.

61. Heap, I. The International survey of herbicide resistant weeds. http://www.weedscience.org/Summary/MOA.aspx?MOAID=10, accessed July 26, 2016.

62. Matsumoto, H. Mode of action of pyrazole herbicides pyrazolate and pyrazoxyfen: HPPD inhibition by the common metabolite. In *New discoveries in agrocemicals*; Clark, J. M., Ohkawa, H., Eds.; American Chemical Society: Washington DC, 2004; pp 161–171.

63. Shimoharada, H.; Tsukamoto, M.; Ikeguchi, M.; Kikugawa, H.; Sano, M.; Kitahara, Y.; Kominami, H.; Okita, T. Benzoylpyrazole compounds and herbicides containing them. WO 2007/069771, June 21, 2007.

64. Williams, K. L.; Tjeerdema, R. S. Hydrolytic activation kinetics of the herbicide benzobicyclon in simulated aquatic systems. *J. Agric. Food Chem.* **2016**, *64*, 4838-4844.

65. Komatsubara, K.; Sekino, K.; Yamada, Y.; Koyanagi, H.; Nakahara, S. Discovery and development of a new herbicide, benzobicyclon. *J. Pestic. Sci.* **2009**, *34*, 113-114.

66. Pallett, K. E.; Cramp, S. M.; Little, J. P.; Veerasekaran, P.; Crudace, A. J.; Slater, A. E. Isoxaflutole: the background of its discovery and the basis of its herbicidal properties. *Pest Manag. Sci.* **2001**, *57*, 133-142.

67. Knudsen, C. G.; Lee, D. L.; Michaely, W. J.; Chin, H.-L.; Nguyen, N. H.; Rusay, R. J.; Cromartie, T. H.; Gray, R.; Lake, B. H.; Fraser, T. E. M.; Cartwright, D. Discovery of the triketone class of HPPD inhibiting herbicides and their relationship to naturally occurring β-triketones. In *Allelopathy in ecological agriculture and forestry. Proceedings of the III international congress on allelopathy in ecological agriculture and forestry*; Narwal, S. S., Hoagland, R. E., Dilday, R. H., Reigosa, M. J., Eds.; Kluwer Academic Publishers: Dordrecht, the Netherlands, 2000; pp 101-111.

68. Penfold, A. R. On the occurrence of a new phenol in the essential oils of the "Leptospermum". *J. Proc. Royal Soc. New South Wales* **1921**, *55*, 49-51.

69. Owens, D. K.; Nanayakkara, N. P.; Dayan, F. E. *In planta* mechanism of action of leptospermone: impact of its physico-chemical properties on uptake, translocation, and metabolism. *J. Chem. Ecol.* **2013**, *39*, 262-270.

70. Porter, N. G.; Wilkins, A. L. Chemical, physical and antimicrobial properties of essential oils of *Leptospermum scoparium* and *Kunzea ericoides*. *Phytochemistry* **1998**, *50*, 407-415.

71. Dayan, F. E.; Singh, N.; McCurdy, C.; Godfrey, C. A.; Larsen, L.; Weavers, R. T.; van Klink, J. W.; Perry, N. B. β-Triketones inhibitors of plant *p*-hydroxyphenylpyruvate dioxygenase: modeling and comparative molecular field analysis of their interactions. *J. Agric. Food Chem.* **2009**, *57*, 5194-5200.

72. Lee, D. L.; Knudsen, C. G.; Michaely, W. J.; Chin, H.-L.; Nguyen, N. H.; Carter, C. G.; Cromartie, T. H.; Lake, B. H.; Shribbs, J. M.; Fraser, T. The structure-activity relationships of the triketon class of HPPD herbicides. *Pestic. Sci.* **1998**, *54*, 377-384.

73. Beaudegnies, R.; Edmunds, A. J. F.; Fraser, T. E. M.; Hall, R. G.; Hawkes, T. R.; Mitchell, G.; Schaetzer, J.; Wendeborn, S.; Wibley, J. Herbicidal 4-hydroxyphenylpyruvate dioxygenase inhibitors – a review of the triketone chemistry story from a Syngenta perspective. *Bioorg. Med. Chem.* **2009**, *17*, 4134-4152.

74. Sandmann, G.; Boger, P.; Kumita, I. Atypical inhibition of phytoene desaturation by 2-(4-chloro-2-nitrobenzoyl)-5,5-dimethylcyclohexane-1,3-dione. *Pestic. Sci.* **1990**, *30*, 353-355.

75. Lee, D. L.; Prysbilla, M. P.; Cromartie, T. H.; Dagarin, D. P.; Howard, S. W.; McLean Provan, W.; Ellis, M. K.; Fraser, T.; Mutter, L. C. The discovery and structural requirements of inhibitors of *p*-hydroxyphenylpyruvate dioxygenase. *Weed Sci.* **1997**, *45*, 601-609.

76. Edmunds, A. J. F.; Morris, J. A. Triketones. In *Modern Crop Protection Compounds, Second Edition, Chapter 4: Herbicides with bleaching properties*; Kramer, W., Schirmer, U., Jeschke, P., Witschel, M., Eds.; Wiley-VCH Verlag GmbH & Co. KgaA: Weinheim, Germany, 2012; pp 235-262.

77. Wu, C.; Huang, J.; Sun, Y.; Yang, D. Mode of action of 4-hydroxyphenylpyruvate dioxygenase inhibition by triketone-type inhibitors. *J. Med. Chem.* **2002**, *45*, 2222-2228.

78. Huang, M.-L.; Zou, J.-W.; Yang, D.-Y.; Ning, B.-Z.; Shang, Z.-C.; Yu, Q.-S. Theoretical studies on tautomerism of benzoylcyclohexane-1,3-dione and its derivatives. *J. Mol. Struct. (Teochem)* **2002**, *589-590*, 321-328.

79. Wu, N.; Jin, Y.; Jin, F.; Tan, Y.; Tao, H.; Zheng, M.; Chen, R.; Liu, K.; Gao, M. Effects of sulcotrione [2-(2-chloro-4-mesylbenzoyl)-cyclohexane-1,3-dione] on enzymes involved in tyrosine catabolism and the extent of the resulting tyrosinemia and its relationship with corneal lesions in rats. *Pestic Biochem. Physiol.* **2011**, *99*, 162-169.

80. Lin, Y.; Wu, C.; Lin, S.; Yang, D. SAR studies of 2-*o*-substituted-benzoyl- and 2-alkanoyl-cyclohexane-1,3-diones as inhibitors of 4-hydroxyphenylpyruvate dioxygenase. *Bioorg. Med. Chem. Lett.* **2000**, *10*, 843-845.

81. Kuo, P.; Shie, T.; Chen, Y.; Lai, J.; Yang, D. Enzyme inhibition potency enhancement by active site metal chelating and hydrogen bonding induced conformation-restricted cyclopropanecarbonyl derivatives. *Bioorg. Med. Chem. Lett.* **2006**, *16*, 6024-6027.

82. Lin, S.; Lin, Y.; Lin, T.; Yang, D. Discovery of a potent, non-triketone type inhibitor of 4-hydroxyphenylpyruvate dioxygenase. *Bioorg. Med. Chem. Lett.* **2000**, *10*, 1297-1298.

83. Lin. Y.; Wu. C.; Lin. S.; Huang. J.; Sun. Y.; Yang. D. SAR studies of 3-cyclopropanecarbonyloxy-2-cyclohexen-1-one as inhibitors of 4-hydroxyphenylpyruvate dioxygenase. *Bioorg. Med. Chem.* **2002**, *10*, 685-690.

84. Huang, J.; Liu, H.; Yang, D. Acylcyclohexanedione derivatives as potential in vivo sequential inhibitors of 4-hydroxyphenylpyruvate dioxygenase and GA_{20} 3β-hydroxylase. *Bioorg. Med. Chem. Lett.* **2003**, *13*, 927-930.

85. Wang, D.; Lin, H.; Cao, R.; Ming, Z.; Chen, T.; Hao, G.; Yang, W.; Yang, G. Design, synthesis and herbicidal activity of novel quinazoline-2,4-diones as 4-hydroxyphenylpyruvate dioxygenase inhibitors. *Pest Manag. Sci.* **2015**, *71*, 1122-1132.

86. Wang, D.; Lin, H.; Cao, R.; Yang, S.; Chen, Q.; Hao, G.; Yang, W.; Yang, G. Synthesis and herbicidal evaluation of triketone-containing quinazoline-2,4-diones. *J. Agric. Food Chem.* **2014**, *62*, 11786-11796.

87. Wang, D.; Lin, H.; Cao, R.; Chen, T.; Wu, F.; Hao, G.; Yang, W.; Yang, G. Synthesis and herbicidal activity of triketone-quinoline hybrids as novel 4-hydroxyphenylpyruvate dioxygenase inhibitors. *J. Agric. Food Chem.* **2015**, *63*, 5587-5596.

88. Wang, D.-W.; Lin, H.-Y.; He, B.; Wu, F.-X.; Chen, T.; Chen, Q.; Yang, W.-C.; Yang, G.-F. An efficient one-pot synthesis of 2-(aryloxyacetyl)cyclohexane-1,3-diones as herbicidal 4-hydroxyphenylpyruvate dioxygenase inhibitors. *J. Agric. Food Chem.* **2016**, *64*, 8986−8993.

89. Grossmann, K.; Ehrhardt, T. On the mechanism of action and selectivity of the corn herbicide topramezone: a new inhibitor of 4-hydroxyphenylpyruvate dioxygenase. *Pest Manag. Sci.* **2007**, *63*, 429-429.

90. Xu, Y.; Lin, H.; Cao, R.; Ming, Z.; Yang, W.; Yang, G. Pyrazolone-quinazolone hybrids: a novel class of human 4-hydroxyphenylpyruvate dioxygenase inhibitors. *Bioorg. Med. Chem.* **2014**, *22*, 5194-5211.

91. Xu, Y.; Lin, H.; Ruan, X.; Yang, S.; Hao, G.; Yang W.; Yang, G. Synthesis and bioevaluation of pyrazole-benzimidazolone hybrids as novel human 4-hydroxyphenylpyruvate dioxygenase inhibitors. *Eur. J. Med. Chem.* **2015**, *92*, 427-438.

92. Claisen, L.; Stock, R. Ueber die einwirkung des hydroxylamins ouf den benzoylaldehyd C_6H_5-CO-CH_2-COH. *Ber. Dtsch. Chem. Ges.* **1891**, *24*, 130-138.

93. van Almsick, A. Hydroxyphenylpyruvate dioxygenase (HPPD) inhibitors: heterocycles. In *Modern Crop Protection Compounds, Second Edition, Chapter 4: Herbicides with bleaching properties*; Kramer, W., Schirmer, U., Jeschke, P., Witschel, M., Eds.; Wiley-VCH Verlag GmbH & Co. KgaA: Weinheim, Germany, 2012; pp 262-276.

94. Lei, K.; Hua, X.-W.; Tao, Y.-Y.; Liu, Y.; Liu, N.; Ma, Y.; Li, Y.-H.; Xu, X.-H.; Kong, C.-H. Discovery of (2-benzoylethen-1-ol)-containing 1,2-benzothiazine derivatives as novel 4-hydroxyphenylpyruvate dioxygenase (HPPD) inbibiting-based herbicide lead compounds. *Bioorg. Med. Chem.* **2016**, *24*, 92-103.

95. Romagni, J. G.; Meazza, G.; Nanayakkara, N. P. D.; Dayan, F. E. The phytotoxic lichen metabolite, usnic acid, is a potent inhibitor of plant *p*-hydroxyphenylpyruvate dioxygenase. *FEBS Lett*. **2000**, *480*, 301-305.

96. Romagni, J. G.; Rosell, R. C.; Nanayakkara, N. P. D.; Dayan, F. E. Ecophysiology and potential mode of action for selected lichen secondary metabolites. In *Allelopathy: chemistry and mode of action of allelochemicals*; Macias, F. A., Galindo, J. C. G., Molinillo, J. M. G., Cutler, H. G., Eds.; CRC Press LLC: Boca Raton, FL, 2000; pp 13-33.

97. Meazza, G.; Scheffler, B. E.; Tellez, M. R.; Rimando, A. M.; Romagni, J. G.; Duke, S. O.; Nanayakkara, D.; Khan, I. A.; Abourashed, E. A.; Dayan, F. E. The inhibitory activity of natural products on plant *p*-hydroxyphenylpyruvate dioxygenase. *Phytochemistry* **2002**, *59*, 281-288.

98. Chiari, M. E.; Tosoni, L.; Joray, M. B.; Diaz Napal, G. N.; Palacios, S. M.; Ruiz, G. M.; Vera, D. M. A.; Carpinella, M. C. The inhibitory activity of plants from central Argentina on *p*-hydroxyphenylpyruvate dioxygenase. Isolation and mechanism of inhibition of a flavanone from *Flourensia oolepis*. *Planta Med.* **2015**, *81*, 1382-1391.

99. Ling, T.; Shiu, S.; Yang, D. Design and synthesis of 3-fluoro-2-oxo-3-phenylpropionic acid derivatives as potent inhibitors of 4-hydroxyphenylpyruvate dioxygenase from pig liver. *Bioorg. Med. Chem.* **1999**, *7*, 1459-1465.

100. Sergeant, M. J.; Harrison, P. J.; Jenkins, R.; Moran, G. R.; Bugg, T. D. H.; Thompson, A. J. Phytotoxic effects of selected *N*-benzyl-benzoylhydroxamic acid metallo-oxygenase inhibitors: investigation into mechanism of action. *New J. Chem.* **2013**, *37*, 3461-3465.

101. Lopez-Ramos, M.; Perruccio, F. HPPD: ligand- and target-based virtual screening on a herbicide target. *J. Chem. Inf. Model.* **2010**, *50*, 801-814.

102. Cho, J. E.; Kin, J. T.; Kim, E.; Ko, Y. K.; Kang, N. S. The structure-based three-dimensional pharmacophore models for *Arabidopsis thaliana* HPPD inhibitors as herbicide. *Bull. Korean Chem. Soc.* **2013**, *34*, 2909-2914.

103. Gomez-Jeria, J. S.; Moreno-Rojas, C. A theoretical study of the inhibition of human 4-hydroxyphenylpyruvate dioxygenase by a series of pyrazalone-quinazolone hybrids. *Pharma Chem.* **2016**, *8*, 475-482.

104. Cardoso Silva, T.; dos Santos Pires, M.; Alves de Castro, A.; da Cunha, E. F. F.; Soares Caetano, M.; Ramalho, T. C. Molecular insight into the inhibition mechanism of plant and rat 4-hydroxyphenylpyruvate dioxygenase by molecular docking and DFT calculations. *Med. Chem. Res.* **2015**, *24*, 3958-3971.

105. Natt, E.; Kida, K.; Odievre, M.; Di Rocco, M.; Scherer, G. Point mutations in the tyrosine aminotransferase gene in tyrosinemia type II. *Proc. Natl. Acad. Sci. U.S.A.* **1992**, *89*, 9297-9301.

106. Angileri, F.; Bergeron, A.; Morrow, G.; Lettre, F.; Gray, G.; Hutchin, T.; Ball, S.; Tanguay, R. M. Geographical and ethnic distribution of mutations of the fumarylacetoacetate hydrolase gene in hereditary tyrosinemia type 1. *J. Inher. Metab. Dis. Rep.* **2015**, *19*, 43-58.

107. Jorquera, R.; Tanguay, R. M. Fumarylacetoacetate, the metabolite accumulating in hereditary tyrosinemia, activates the ERK pathway and induces mitotic abnormalities and genomic instability. *Hum. Mol. Genet.* **2001**, *10*, 1741-1752.

108. Geminiani, M.; Gambassi, S.; Millucci, L.; Lupetti, P.; Collodel, G.; Mazzi, L.; Frediani, B.; Braconi, D.; Mazzocchi, B.; Laschi, M.; Bernardini, G.; Santucci, A. Cytoskeleton aberrations in alkaptonuric chondrocytes. *J. Cell Physiol.* [Accepted manuscript online]. DOI: 10.1002/jcp.25500. Published Online: July 25, 2016.

109. Millucci, L.; Giorgetti, G.; Viti, C.; Ghezzi, L.; Gambassi, S.; Braconi, D.; Marzocchi, B.; Paffetti, A.; Lupetti, P.; Bernardini, G.; Orlandini, M.; Santucci, A. Chondroptosis in alkaptonuric cartilage. *J. Cell Physiol.* **2015**, *230*, 1148-1157.

110. Braconi, D.; Bernardini, G.; Bianchini, C.; Laschi, M.; Millucci, L.; Amato, L.; Tinti, L.; Serchi, T.; Chellini, F.; Spreafico, A.; Santucci A. Biochemical and proteomic characterization of alkaptonuric chondrocytes. *J. Cell Physiol.* **2012**, *227*, 3333-3343.

111. Laschi, M.; Tinti, L.; Braconi, D.; Millucci, L.; Ghezzi, L.; Amato, L.; Selvi, E.; Spreafico, A.; Bernardini, G.; Santucci, A. Homogentisate 1,2 dioxygenase is expressed in human osteoarticular cells: implications in alkaptonuria. *J. Cell Physiol.* **2012**, *227*, 3254-3257.

112. Millucci, L.; Ghezzi, L.; Paccagnini, E.; Giorgetti, G.; Viti, C.; Braconi, D.; Laschi, M.; Geminiani, M.; Soldani, P.; Lupetti, P.; Orlandini, M.; Benvenuti, C.; Perfetto, C.; Spreafico, A.; Bernardini, G.; Santucci, A. Amyloidosis, inflammation, and oxidative stress in the heart of an alkaptonuric patient. *Mediat. Inflamm.* **2014**, 258471.

113. Millucci, L.; Ghezzi, L.; Braconi, D.; Laschi, M.; Geminiani, M.; Amato, L.; Orlandini, M.; Benvenuti, C.; Bernardini, G.; Santucci, A. Secondary amyloidosis in an alkaptonuric aortic valve. *Int. J. Cardiol.* **2014**, *172*, e121-e123.

114. Bernardini, G.; Laschi, M.; Geminiani, M.; Braconi, D.; Vannuccini, E.; Lupetti, P.; Manetti, F.; Millucci, L.; Santucci, A. Homogentisate 1,2 dioxygenase is expressed in brain: implications in alkaptonuria. *J. Inherit. Metab. Dis.* **2015**, *38*, 807-14.

115. Wolff, F.; Biaou, I.; Koopmansch, C.; Vanden Bossche, M.; Pozdzik, A.; Roumeguère, T.; Cotton, F. Renal and prostate stones composition in alkaptonuria: a case report. *Clin. Nephrol.* **2015**, *84*, 339-342.

116. ClinicalTrials.gov, a service of the U. S. National Institutes of Health. https://clinicaltrials.gov/ct2/results?term=alkaptonuria+nitisinone&Search=Search, accessed August 25, 2016.

117. Lewis, R. W.; Botham, J. W. A review of the mode of toxicity and relevance to humans of the triketone herbicide 2-(4-methylsulfonyl-2-nitrobenzoyl)-1,3-cyclohexanedione. *Crit. Rev. Toxicol.* **2013**, *43*, 185-199.

118. Lock, E. A.; Gaskin, P.; Ellis, M. K.; McLean Provan, W.; Robinson, M.; Smith, L. L. Tissue distribution of 2-(2-nitro-4-trifluoromethylbenzoyl)-cyclohexane-1,3-dione (NTBC) and its effect on enzymes involved in tyrosine catabolism in the mouse. *Toxicology* **2000**, *144*, 179-197.

119. Lock, E. A.; Gaskin, P.; Ellis, M.; Provan, W. M.; Smith, L. L. Tyrosinemia produced by 2-(2-nitro-4-trifluoromethylbenzoyl)-cyclohexane-1,3-dione (NTBC) in experimental animals and its relationship to corneal injury. *Toxicol. Appl. Pharmacol.* **2006**, *215*, 9-16.

120. Gamelin, L.; Turcant, A.; Ganiere-Monteil, C.; Harry, P. Toxicité des tricétones: rapport de 2 cas d'intoxication à la sulcotrione du Cap d'Angers et revue de la littérature. *Infotox Bull. Soc. Toxicol. Clin.* **2006**, *23*, 3-6.

121. Boels, D.; Ganiere-Monteil, C.; Turcant, A.; Bretaudeau, M.; Harry, P. Triketone toxicity: a report on two cases of sulcotrione poisoning. *Hum. Exp. Toxicol.* **2013**, *32*, 778-782.

122. Hall, M. G.; Wilks, M. F.; McLean Provan, W.; Eksborg, S.; Lumholtz, B. Pharmacokinetics and pharmacodynamics of NTBC (2-(2-nitro-4-fluoromethylbenzoyl)-1,3-cyclohexanedione) and meostrione, inhibitors of 4-hydroxyphenyl pyruvate dioxygenase (HPPD) following a single dose to healthy male volunteers. *Br. J. Clin. Pharmacol.* **2001**, *52*, 169-177.

123. Lock, E.; Ranganath, L. R.; Timmis, O. The role of nitisinone in tyrosine pathway disorders. *Curr. Rheumatol. Rep.* **2014**, *16*, 457.

124. Davison, A. S.; Milan, A. M.; Gallagher, J. A.; Ranganath, L. R. Acute fatal metabolic complications in alkaptonuria. *J. Inherit. Metab. Dis.* **2016**, *39*, 203-210.

125. European Food Safety Authority. Conclusion on the peer review of the pesticide risk assessment of the active substance tembotrione. *EFSA J.* **2013**, *11*, 3131.

126. Zunec, S.; Kasuba, V.; Pavicic, I.; Marjanovic, A. M.; Tariba, B.; Milic, M.; Kopjar, N.; Pizent, A.; Vrdoljak, A. L.; Rozgaj, R.; Zeljezic, D. Assessment of oxidative stress responses and the cytotoxic and genotoxic potential of the herbicide tembotrione in HepG2 cells. *Food Chem. Toxicol.* **2016**, *94*, 64-74.

127. Batisson, I.; Crouzet, O.; Besse-Hoggan, P.; Sancelme, M.; Mangot, J.-F.; Mallet, C.; Bohatier, J. Isolation and characterization of mesotrione-degrading *Bacillus* sp. from soil. *Environ. Pollut.* **2009**, *157*, 1195-1201.

128. Romdhane, S.; Devers-Lamrani, M.; Calvayrac, C.; Rocaboy-Faquet, E.; Riboul, D.; Cooper, J. F.; Barthelmebs, L. Isolation and characterization of *Bradyrhizobium* sp. SR1 degrading two β-triketone herbicides. *Environ. Sci. Pollut. Res. Int.* **2016**, *23*, 4138-4148.

129. Antonenko, A. M.; Blagaia, A. V.; Omelchuck, S. T.; Korshun, M. M.; Vavrinevych, H. P.; Milohov, D. S.; Pelo, I. M.; Bojar, I. Mechanism of action of 4-hydroxyphenylpyruvate dioxygenase inhibitor herbicide on homoterm animals and humans. *J. Pre-Clin. Clin. Res.* **2015**, *9*, 145-150.

130. Lewis, K. A.; Tzilivakis, J.; Warner, D.; Green, A. An international database for pesticide risk assessments and management. *Hum. Ecol. Risk Assess.* **2016**, *22*, 1050-1064. http://sitem.herts.ac.uk/aeru/ppdb/en/index.htm, accessed August 12, 2016.

131. Moran, G. R.; He, P. Treatment of microbial infections with compounds that inhibit 4-hydroxyphenylpyruvate dioxygenase. US 2010/227936 A1, September 9, 2010.

132. Christoph, F.; Kaulfers, P.-M.; Stahl-Biskup, E. A comparative study of the *in vitro* antimicrobial activity of tea tree oils *s.l.* with special reference to the activity of β-triketones. *Planta Med.* **2000**, *66*, 556-560.

133. van Klink, J. W.; Larsen, L.; Perry, N. B.; Weavers, R. T.; Cook, G. M.; Bremer, P. J.; MacKenzie, A. D.; Kirikae, T. Triketones active againts antibiotic-resistant bacteria: synthesis, structure-activity relationships, and mode of action. *Bioorg. Med. Chem.* **2005**, *13*, 6651-6662.

134. Reichling, J.; Koch, C.; Stahl-Biskup, E.; Sojka, C.; Schnitzler, P. Virucidal activity of a β-triketone-rich essential oil of *Leptospermum scoparium* (Manuka oil) against HSV-1 and HSV-2 in cell culture. *Planta Med.* **2005**, *71*, 1123-1127.

135. Carroll, A. R.; Avery, V. M.; Duffy, S.; Forster, P. I.; Guymer, G. P. Watsonianone A-C, anti-plasmodial β-triketones from the Australian tree, *Corymbia watsoniana*. *Org. Biomol. Chem.* **2013**, *11*, 453-458.

136. Sterkel, M.; Perdomo, H. D.; Guizzo, M. G.; Barletta, A. B. F.; Nunes, R. D.; Dias, F. A.; Sorgine, M. H. F.; Oliveira, P. L. Tyrosine detoxification is an essential trait in the life history of blood-feeding arthropods. *Curr. Biol.* **2016**, *26*, 2188–2193.

137. Travis, K. Z.; Posner, J. Use of HPPD inhibitors in the treatment of depression and/or withdrawal symptoms associated with addictive drugs. WO 2008/020150, February, 21, 2008.

138. Pickford, L.; Meya, U.; Moran, M. Treatment of restless leg syndrome and sleep disorders. WO 2010/54273, May 14, 2010.

139. Doe, J. E.; Sturgess, N. C.; Travis, K. Z. Use of 2-(2-nitro-4-trifluoromethylbenzoyl)-1,3-cyclohexanedione in the treatment of Parkinson's disease. WO 2006/090177, August 31, 2006.

140. Biotie therapies corp. Stock exchange release. 23 November 2011, http://www.biotie.com/investors/releases/pr-story.aspx?ResultPageURL=http://cws.huginonline.com/B/132030/PR/201111/1565991.xml, accessed August 17, 2016

141. Nitisinone for type 1B oculocutaneous albinism, https://clinicaltrials.gov/ct2/show/NCT01838655, accessed August 18, 2016.

142. Onojafe, K. F.; Adams, D. R.; Simeonov, D. R.; Zhang, J.; Chan, C.; Bernardini, I. M.; Sergeev, Y. V.; Dolinska, M. B.; Alur, R. P.; Brilliant, M. H.; Gahl, W. A.; Brooks, B. P. Nitisinone improves eye and skin pigmentation defects in a mouse model of oculocutaneous albinism. *J. Clin. Invest.* **2011**, *121*, 3914-3923.

143. Brooks, B. P.; Gahl, W. A. The nitisinone for the treatment of oculocutaneous/ocular albinism and for increasing pigmentation. WO 2011/106655, September 1, 2011.

144. Manga, P.; Orlow, S. J. Informed reasoning: repositioning of nitisinone to treat oculocutaneous albinism. *J. Clin. Invest.* **2011**, *121*, 3828-3831.

Table 2. Structures of HPPD and its complexes stored in the protein data bank.

PDB entry[a] Release date Resolution Reference	Organism/Expression system	Chain: Solved sequence[b]	Ligand Cofactor Coordination	Binding mode[c]
5EC3 2015-11-18 2.1 Å Unpublished results[d]	*H. sapiens* *E. coli* BL21-Gold(DE3)pLysS AG	A: 9-384	Holoenzyme Co(II) distorted five-coordinated	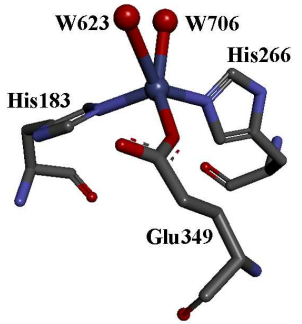
3ISQ 2009-09-15 1.75 Å Unpublished results[e]	*H. sapiens* *E. coli*	A: 9-384	Holoenzyme Co(II) distorted five-coordinated	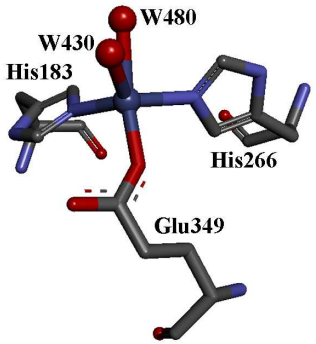

1SP8 2004-09-21 2.0 Å 24	*Z. mais* *E. coli* BL21(DE3)	A: 36-248, 257-431 B: 34-248, 256-432 C: 37-247, 257-431 D: 34-248, 255-432	Holoenzyme Fe(II) octahedral	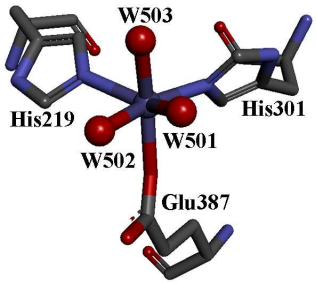
1SP9 2004-09-21 3.0 Å 24	*A. thaliana* *E. coli*	A: 33-106, 117-193, 202-210, 216-251, 263-428 B: 33-106, 117-193, 202-210, 216-254, 263-437	Holoenzyme Fe (iron binding site not resolved at 3.0 Å)	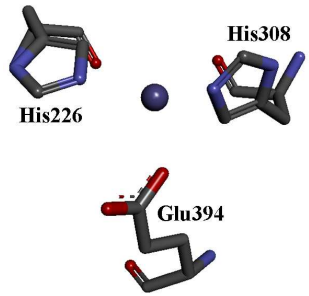

1SQD 2004-08-17 1.8 Å 23	*A. thaliana* *E. coli* BL21(DE3)	A: 14-173, 180-233, 242-266, 270-382, 390-410	Holoenzyme Fe or Co octahedral	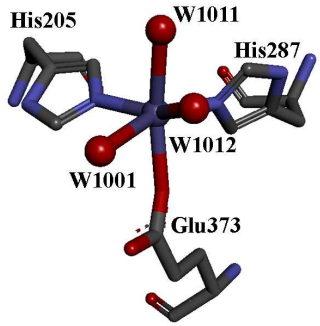
1SQI 2004-08-17 2.15 Å 23	*R. norvegicus* *E. coli* BL21(DE3)	A: 8-212, 224-244, 250-366 B: 7-210, 224-244, 250-366	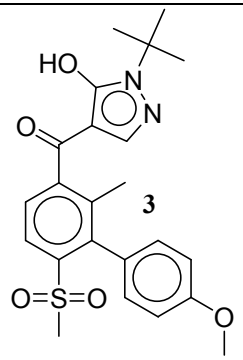 **3** Fe or Co octahedral	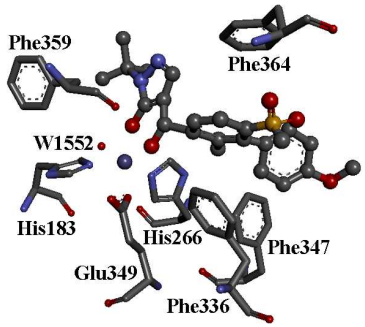

1TFZ 2004-08-17 1.8 Å 23	*A. thaliana* *E. coli* BL21(DE3)	A: 15-172, 180-230, 242-266, 270-381, 391-408	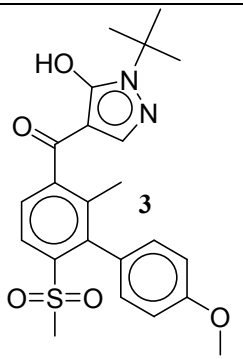 **3** Fe or Co octahedral	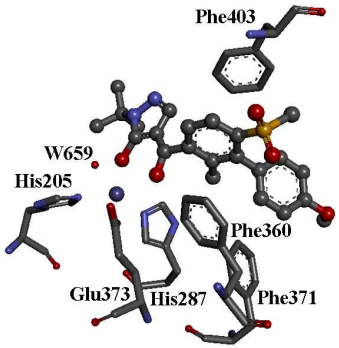
1TG5 2004-08-17 1.9 Å 23	*A. thaliana* *E. coli* BL21(DE3)	A: 14-173, 179-230, 241-267, 270-380, 390-410	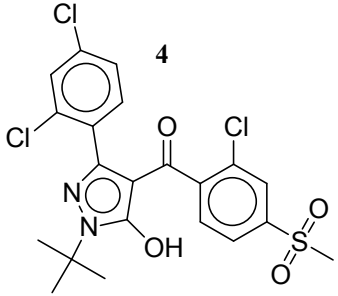 **4** Fe or Co octahedral	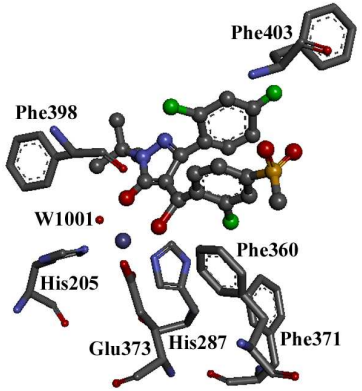

5CTO 2015-08-26 2.62 Å Unpublished results[f]	*A. thaliana* *E. coli* BL21-Gold(DE3)pLysS AG	A: 30-107, 115-193, 201-211, 216-253, 263-285, 290-403, 411-434 B: 30-107, 115-193, 201-211, 215-253, 263-287, 290-403, 411-434 C: 30-107, 116-193, 201-211, 216-253, 264-287, 290-402, 412-434 D: 30-107, 115-193, 201-211, 215-253, 263-287, 290-403, 411-434	**14** 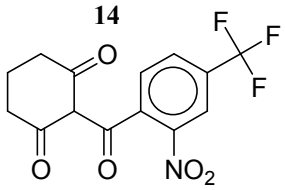 **14** Iron octahedral	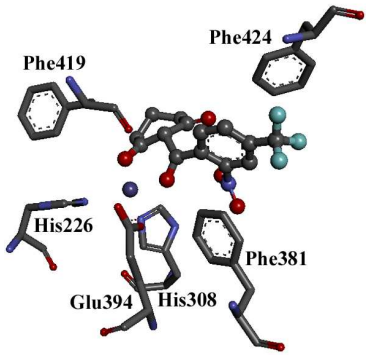

5DHW 2016-09-07 2.62 Å Unpublished results[g]	*A. thaliana* *E. coli* BL21(DE3)	A: 30-107, 115-193, 202-211, 215-253, 263-287, 290-403, 411-434 B: 30-106, 114-193, 202-210, 215-253, 262-287, 290-403, 411-436	**15** 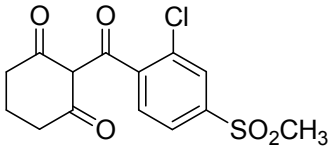 **15** Iron octahedral	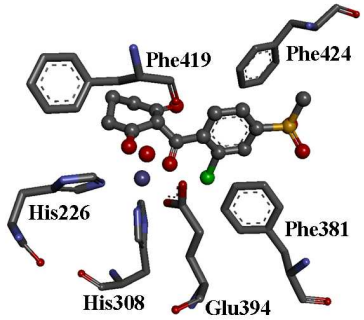
1T47 2004-06-15 2.50 Å 25	*Streptomyces avermitilis* *E. coli* BL21(DE3)	A: 16-377 B: 16-377	**14** 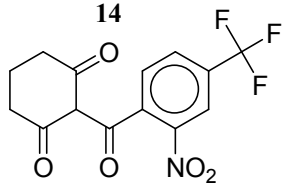 **14** Fe(II) distorted squared pyramidal	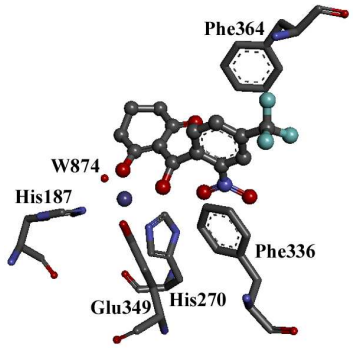

1CJX 2000-04-26 2.4 Å 26	*P. fluorescens* *P. fluorescens*	A: 4-356 B: 4-356 C: 4-356 D: 4-356	Acetate Fe(III) distorted tetrahedral	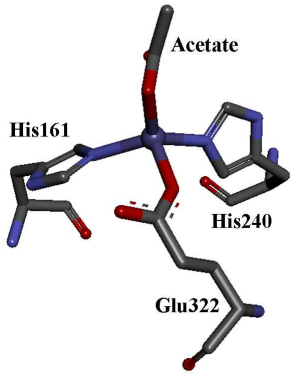

[a]All the structures have been obtained by X-ray diffraction.

[b]HPPD chains (A, B, C, and D) and their solved sequence (i.e., the amino acid sequence listed in the PDB structure) are reported.

[c]Graphical representations of the binding mode of iron ions, coordinated water, and inhibitors within the HPPD binding site. Pictures have been elaborated with Discovery Studio 3.0 Visualizer software (Accelrys Software, Inc.) by the corresponding PDB files.

[d]Yang, W. C.; Yang, G. F. Structural insight into the catalyitc mechanism of human 4-hydroxyphenylpyruvate dioxygenase. Unpublished results.

[e]Pilka, E. S.; Shafqat, N.; Cocking, R.; Bray, J. E.; Krojer, T.; Pike, A. C. W.; von Delft, F.; Yue, W. W.; Arrowsmith, C. H.; Weigelt, J.; Edwards, A.; Bountra, C.; Oppermann, U.; Kavanagh, K. L. Crystal structure of human 4-hydroxyphenylpyruvate dioxygenase. Unpublished results.

[f]Yang, W. C.; Yang, G. F. Crystal structure of *Arabidopsis thaliana* HPPD complexed with NTBC. Unpublished results.

[g]Yang, W. C.; Yang, G. F. Crystal structure of *Arabidopsis thaliana* HPPD complexed with sulcotrione. Unpublished results.

Table 1. Reviewed sequences of HPPD stored within the UniProt Knowledgebase (alphabetical order)

UniProt identifier	Organism's scientific name
P93836	*Arabidopsis thaliana*
Q5EA20	*Bos taurus*
Q60Y65	*Caenorhabditis briggsae*
Q22633	*Caenorhabditis elegans*
Q1E803	*Coccidioides immitis* (strain RS)
P0CW94	*Coccidioides posadasii* (strain C735)
E9CWP5	*Coccidioides posadasii* (strain RMSCC 757)
Q6TGZ5	*Danio rerio*
O23920	*Daucus carota*
Q76NV5	*Dictyostelium discoideum*
P32754	*Homo sapiens*
O48604	*Hordeum vulgare*
P69053	*Legionella pneumophila* (strain Corby)
Q5ZT84	*Legionella pneumophila subsp. pneumophila* (strain Philadelphia 1, ATCC 33152)
Q96X22	*Magnaporthe oryzae* (strain 70-15, ATCC MYA-4617)
P49429	*Mus musculus*
Q872T7	*Neurospora crassa* (strain ATCC 24698)
Q9ARF9	*Plectranthus scutellarioides*
Q9I576	*Pseudomonas aeruginosa* (strain ATCC 15692)

P80064	*Pseudomonas fluorescens* (strain P.J. 874)
P32755	*Rattus norvegicus*
Q53586	*Streptomyces avermitilis* (strain ATCC 31267)
Q9S2F4	*Streptomyces coelicolor* (strain ATCC BAA-471)
Q02110	*Sus scrofa*
Q27203	*Tetrahymena thermophila*
Q5BKL0	*Xenopus tropicalis*
Q6CDR5	*Yarrowia lipolytica* (strain CLIB 122)
O42764	*Zymoseptoria tritici*

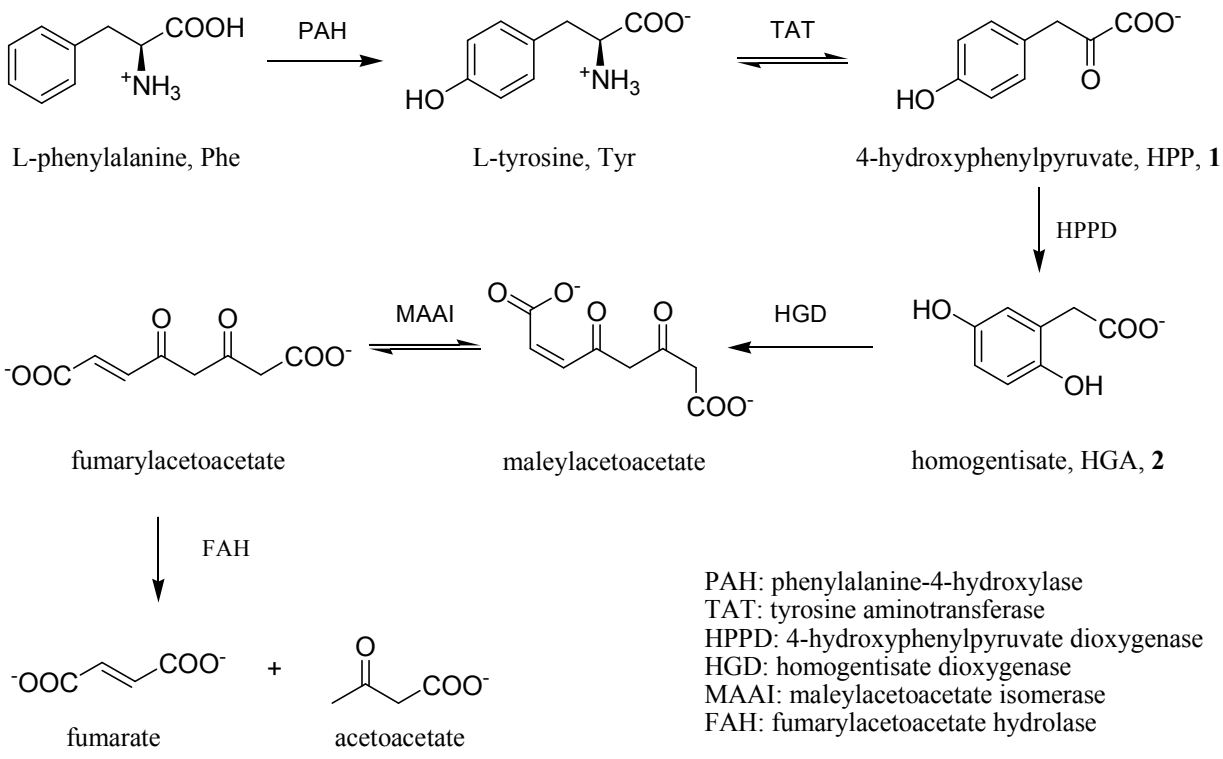

Figure 1.

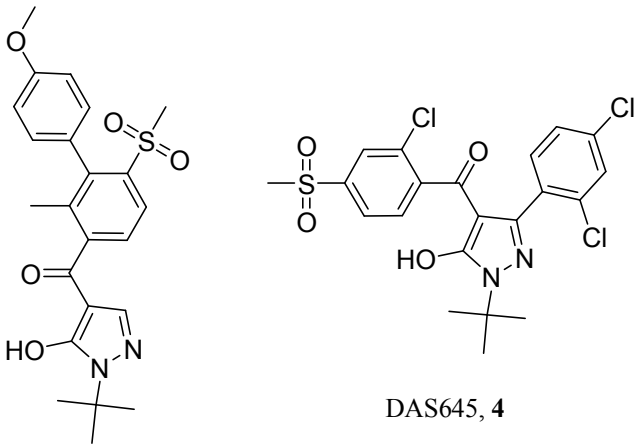

Figure 2.

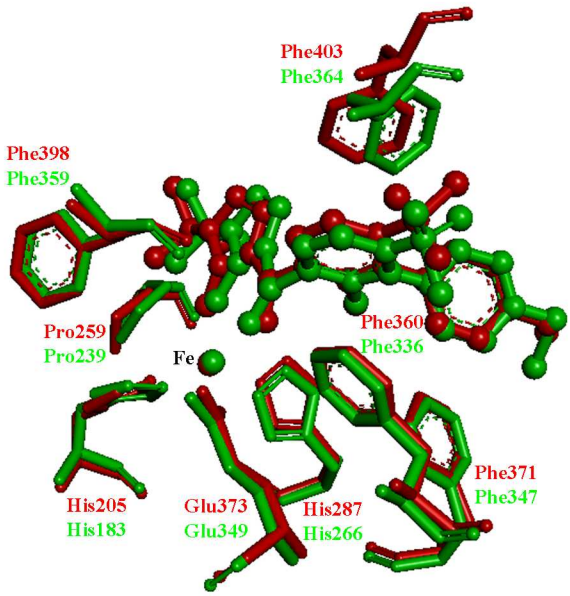

Figure 3.

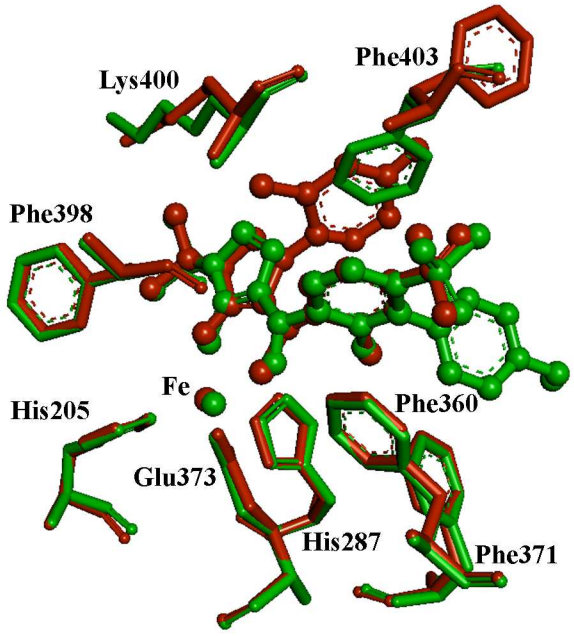

Figure 4.

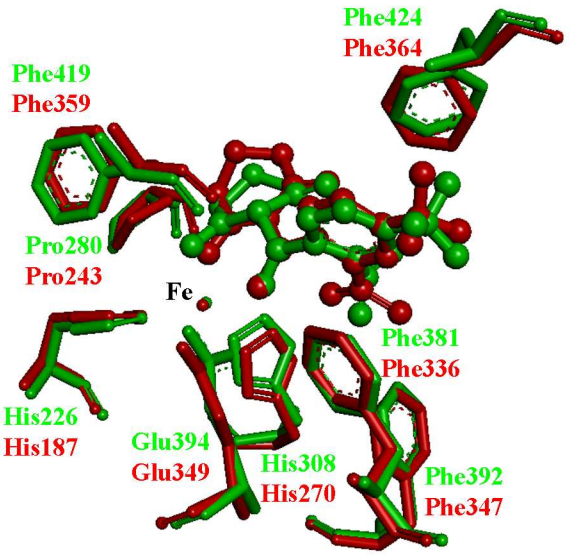

Figure 5.

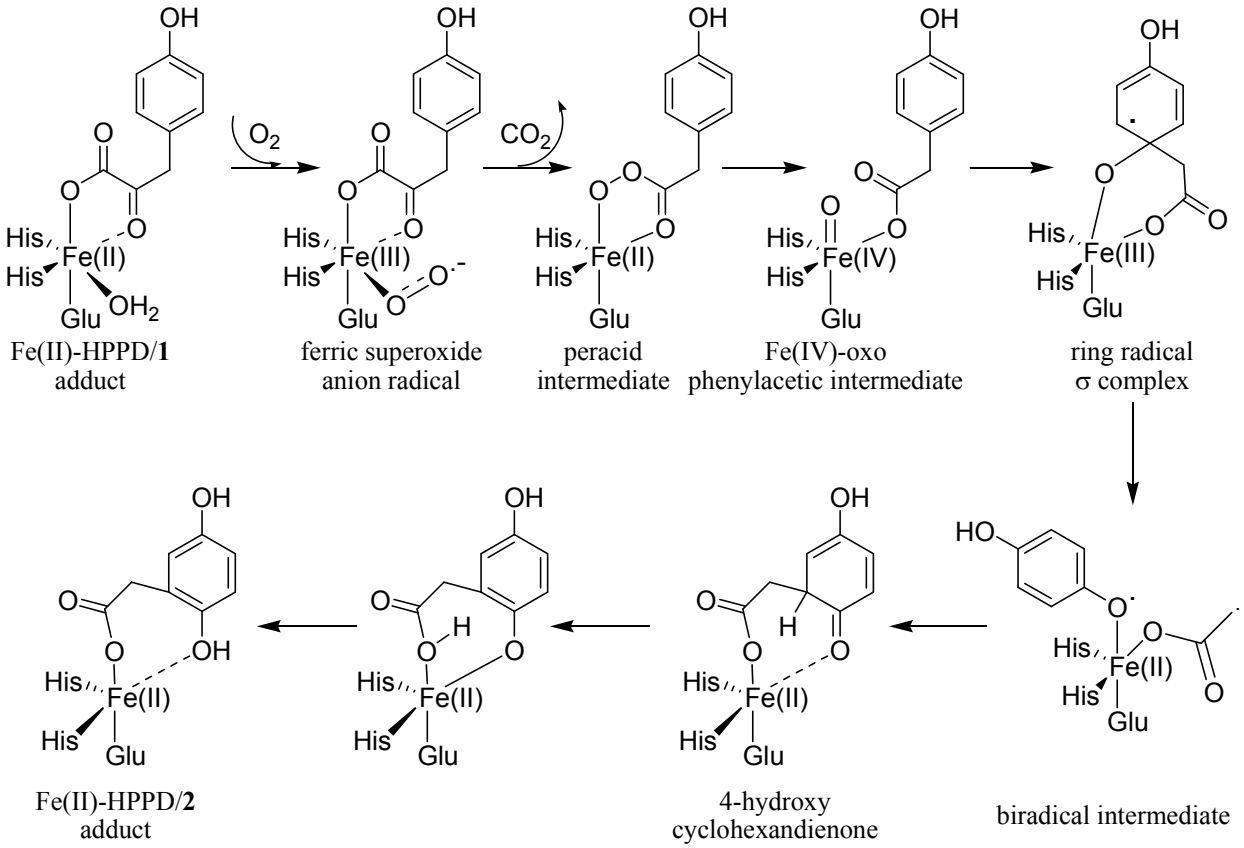

Figure 6.

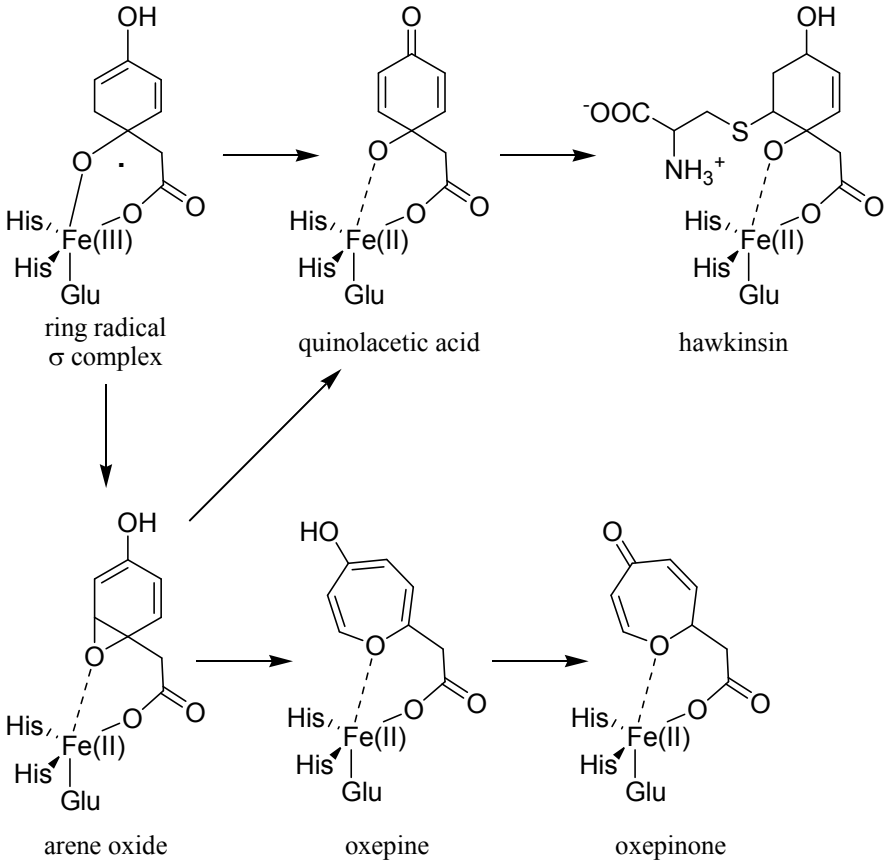
OH
O
His
Fe(III)
His
Glu
ring radical
σ complex
quinolacetic acid
-OOC
S
NH3+
hawkinsin
HO
arene oxide
oxepine
oxepinone

Figure 7.

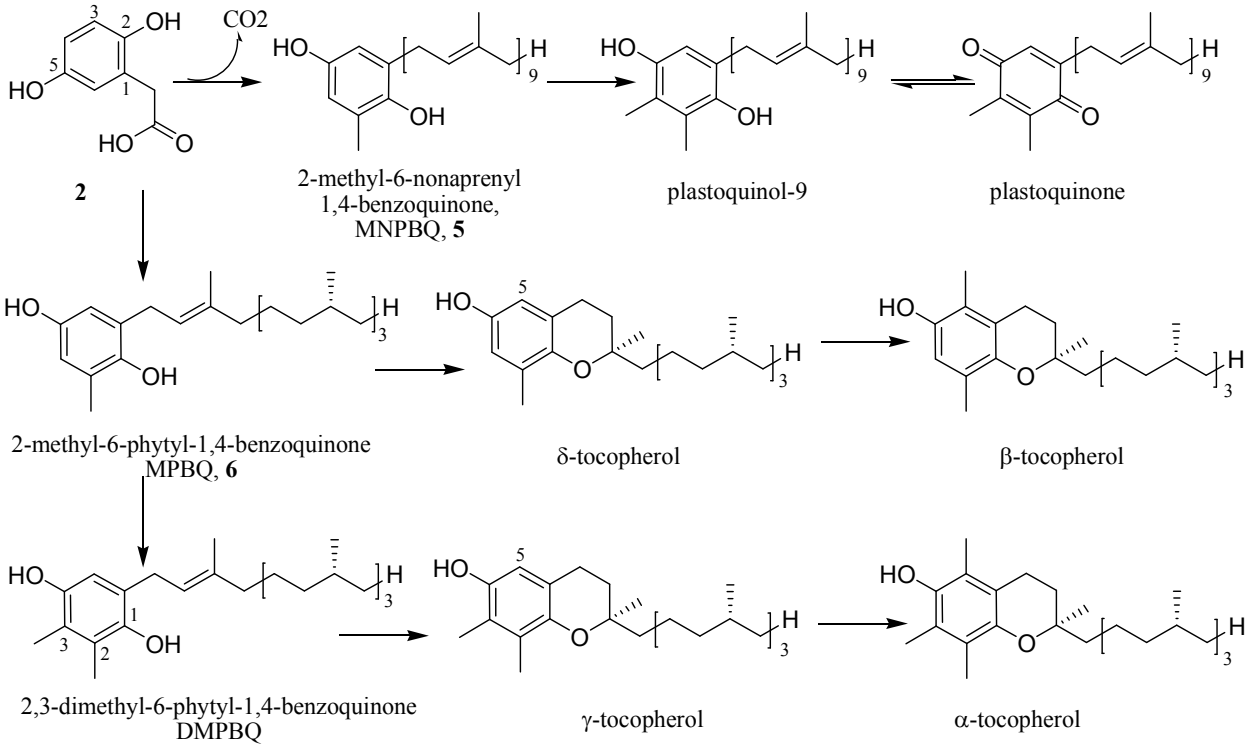

Figure 8.

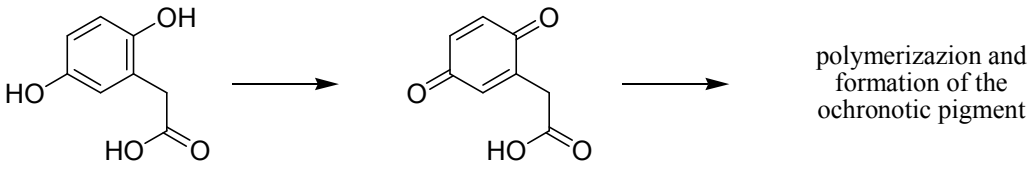

Figure 9.

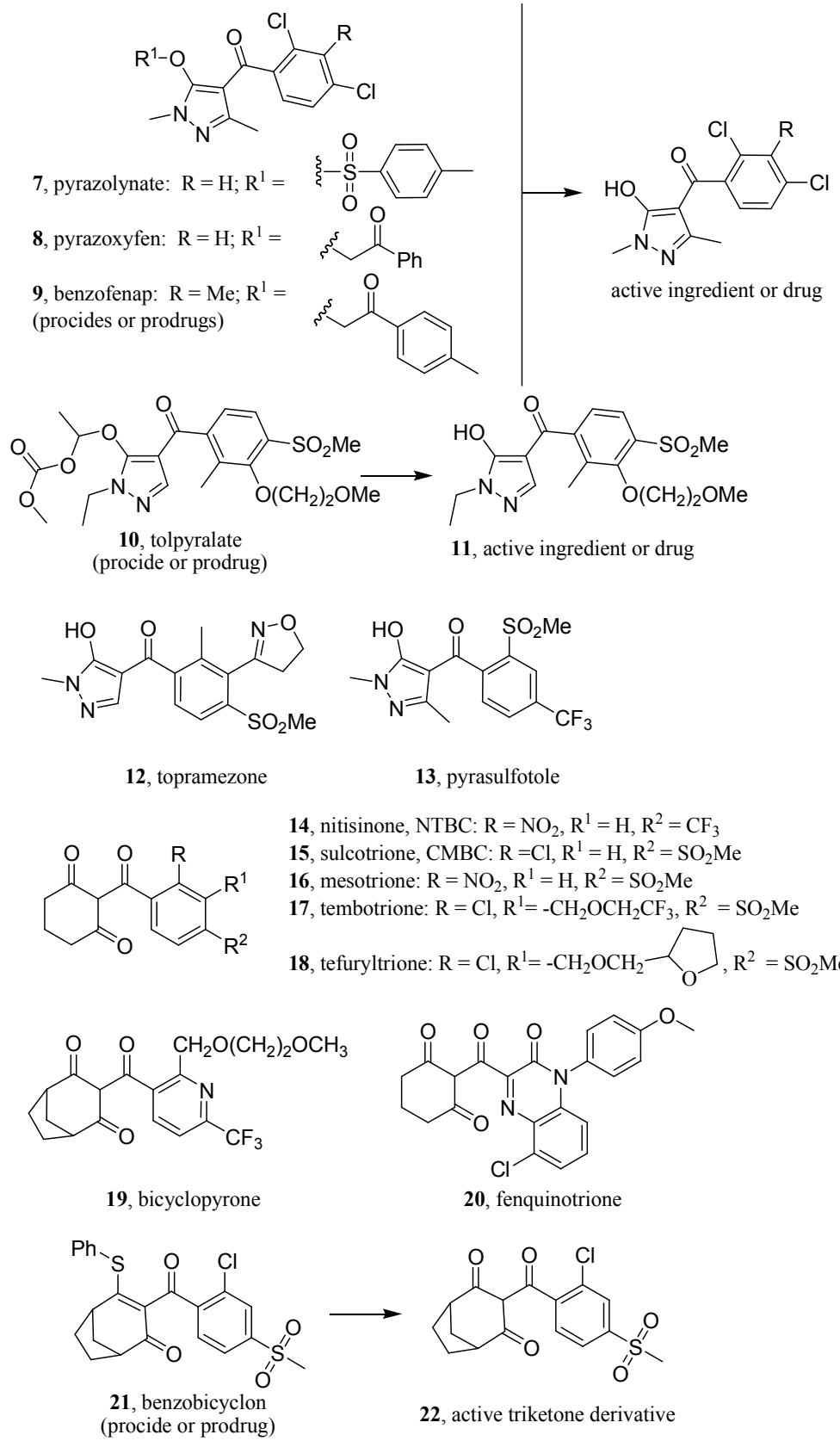
7, pyrazolynate: R = H; R1 =
8, pyrazoxyfen: R = H; R1 =
9, benzofenap: R = Me; R1 =
(procides or prodrugs)
active ingredient or drug
10, tolpyralate
(procide or prodrug)
11, active ingredient or drug
12, topramezone
13, pyrasulfotole
14, nitisinone, NTBC: R = NO2, R1 = H, R2 = CF3
15, sulcotrione, CMBC: R =Cl, R1 = H, R2 = SO2Me
16, mesotrione: R = NO2, R1 = H, R2 = SO2Me
17, tembotrione: R = Cl, R1= -CH2OCH2CF3, R2 = SO2Me
18, tefuryltrione: R = Cl, R1= -CH2OCH2
, R2 = SO2Me
19, bicyclopyrone
20, fenquinotrione
21, benzobicyclon
(procide or prodrug)
22, active triketone derivative

Figure 10.

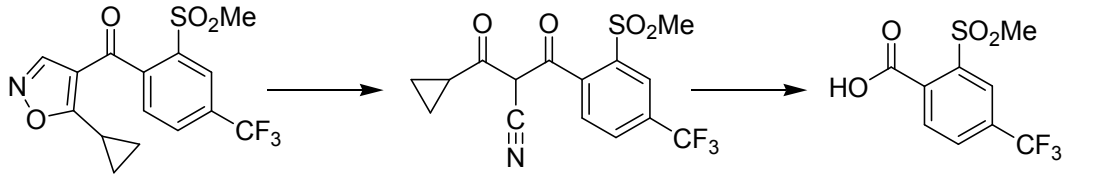

isoxaflutole, **23**
prodrug or procide

diketonitrile, **24**
drug

inactive metabolite, **25**

Figure 11.

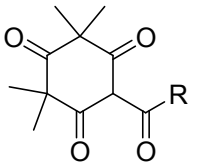

leptospermone, **26**: R =
IC_{50} = 11800 nM

grandiflorone, **27**: R =
IC_{50} = 750 nM

28: R =
IC_{50} = 19 nM

Figure 12.

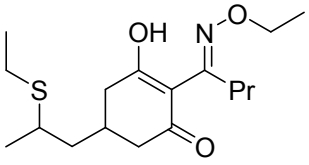

sethoxydim, **29**

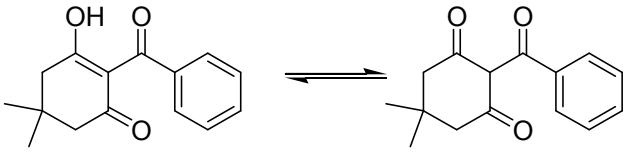

benzoyl dimedone, **30**

Figure 13.

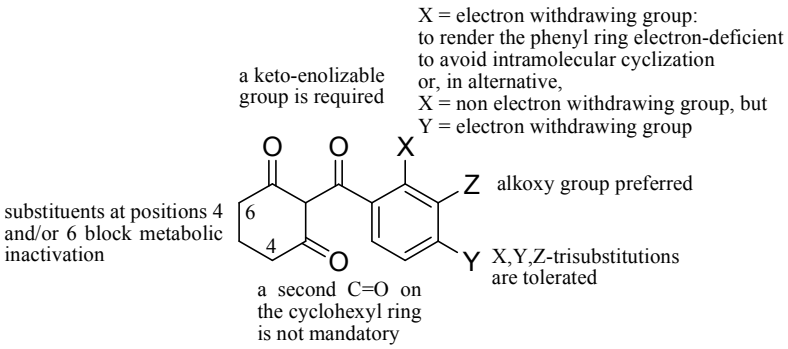

Figure 14.

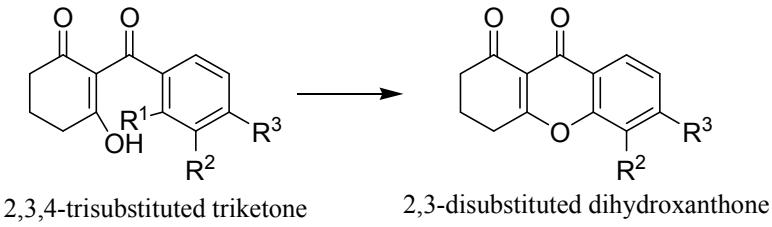

Figure 15.

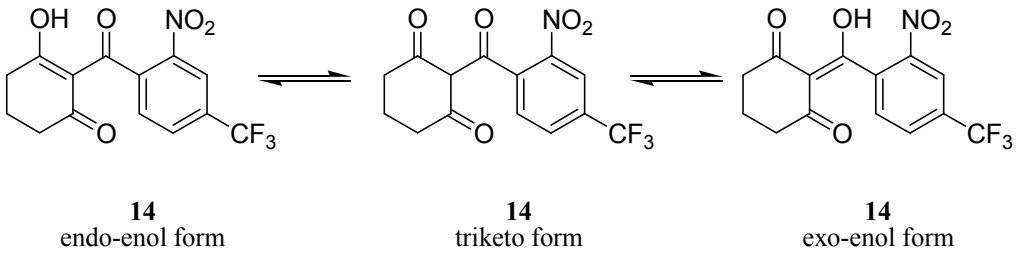

Figure 16.

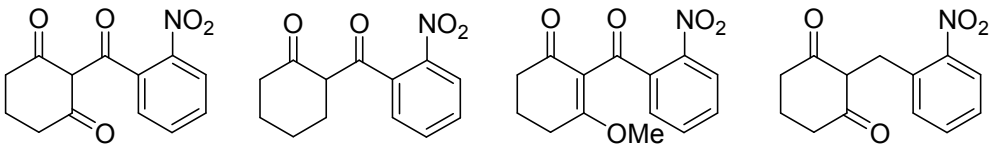

31 0.16 μM **32** 0.70 μM **33** 5.2 μM **34** 126 μM

Figure 17.

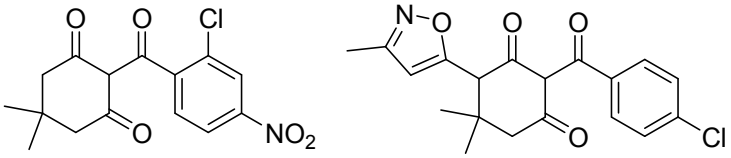

35 IC_{50} = 36 nM **36** IC_{50} = 60 nM

Figure 18.

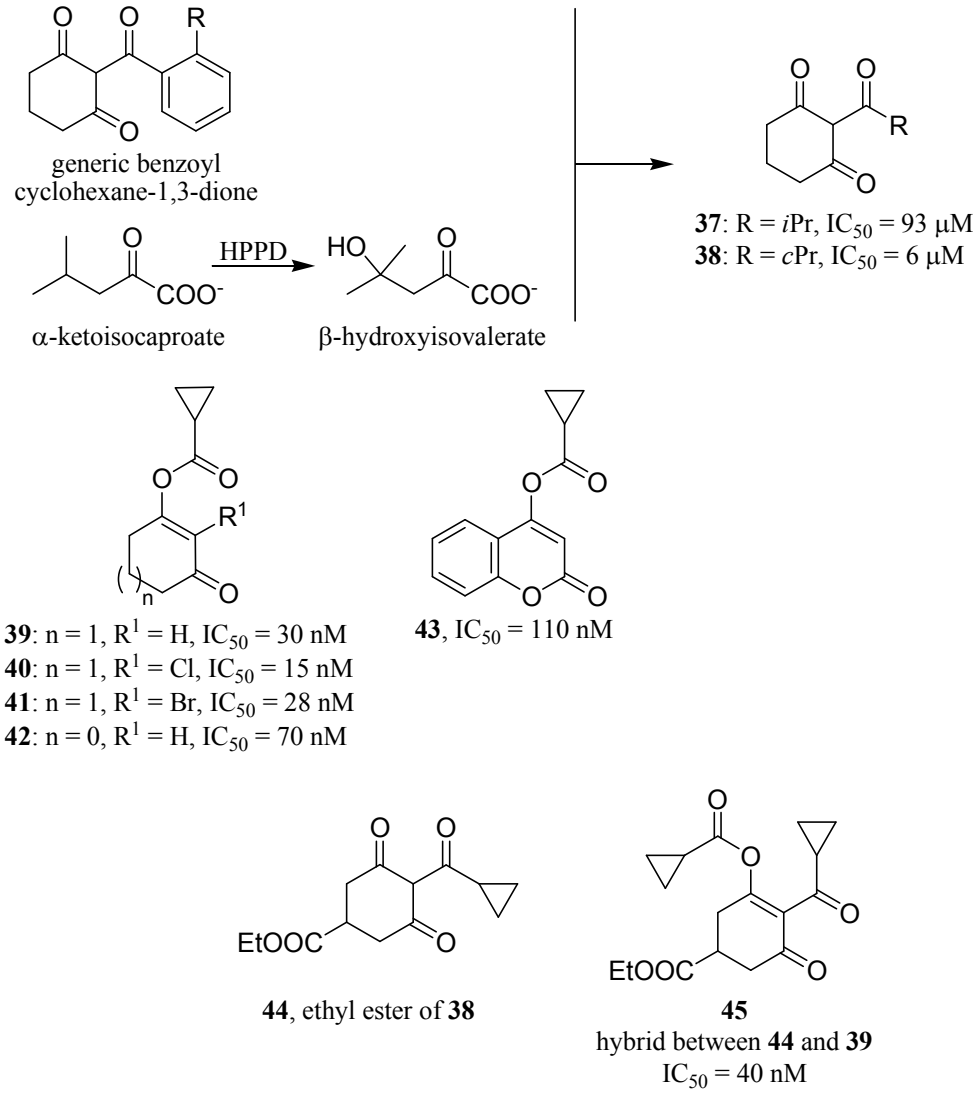

Figure 19.

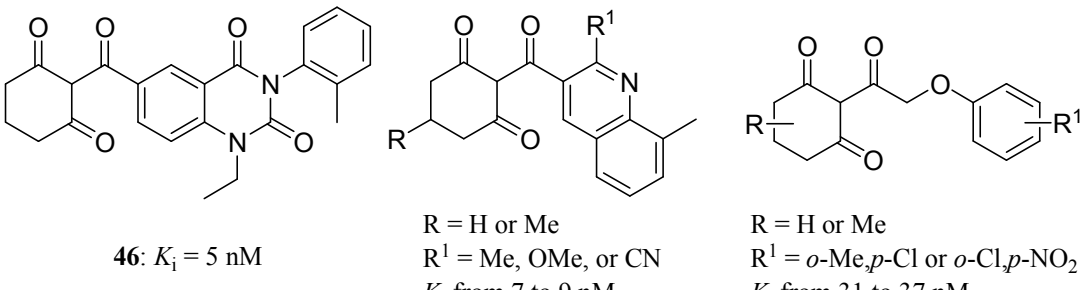

Figure 20.

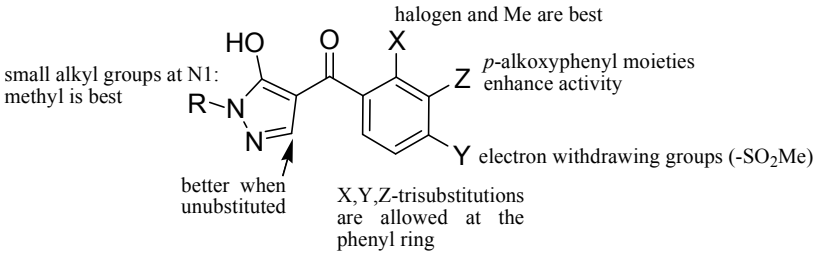

Figure 21.

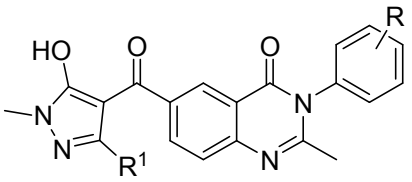

1) first series of pyrazolo-quinazolones
methylated at the C3 of the pyrazole:
R = *o*-F or *o*-Cl, R^1 = Me; best $K_i \approx 80$ nM
2) second generation pyrazolo-quinazolones
unsubstituted at the C3 of the pyrazole:
R = *m*-halogen, or *m*-Me, or *m*-OMe
K_i from 10 to 34 nM

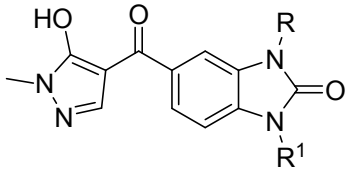

pyrazolo-benzimidazoles
R = Me, Et, or Pr
R^1 = Et, Pr, or *i*Pr
K_i from 21 to 77 nM

Figure 22.

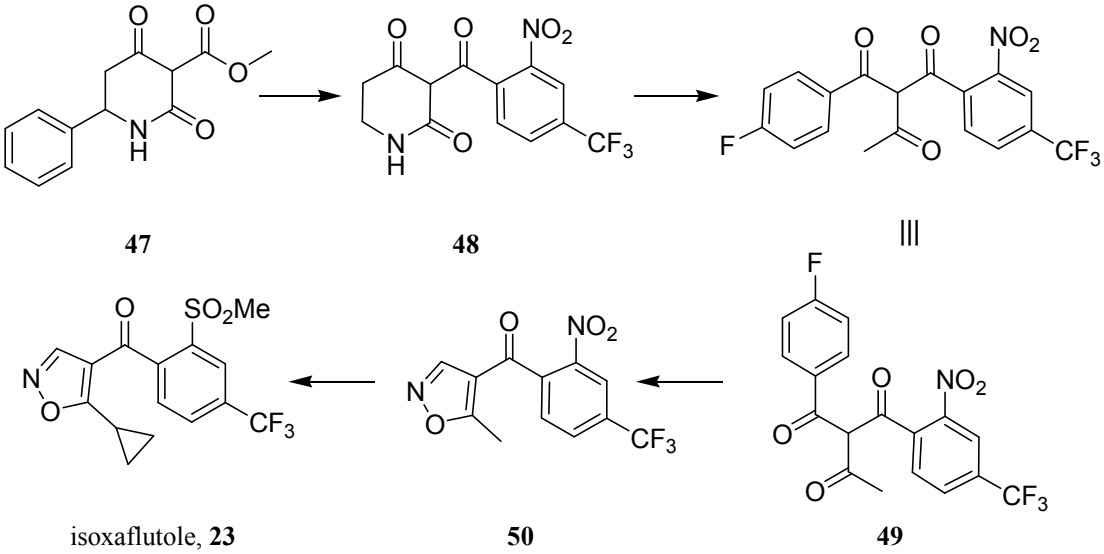

47 **48** III

isoxaflutole, **23** **50** **49**

Figure 23.

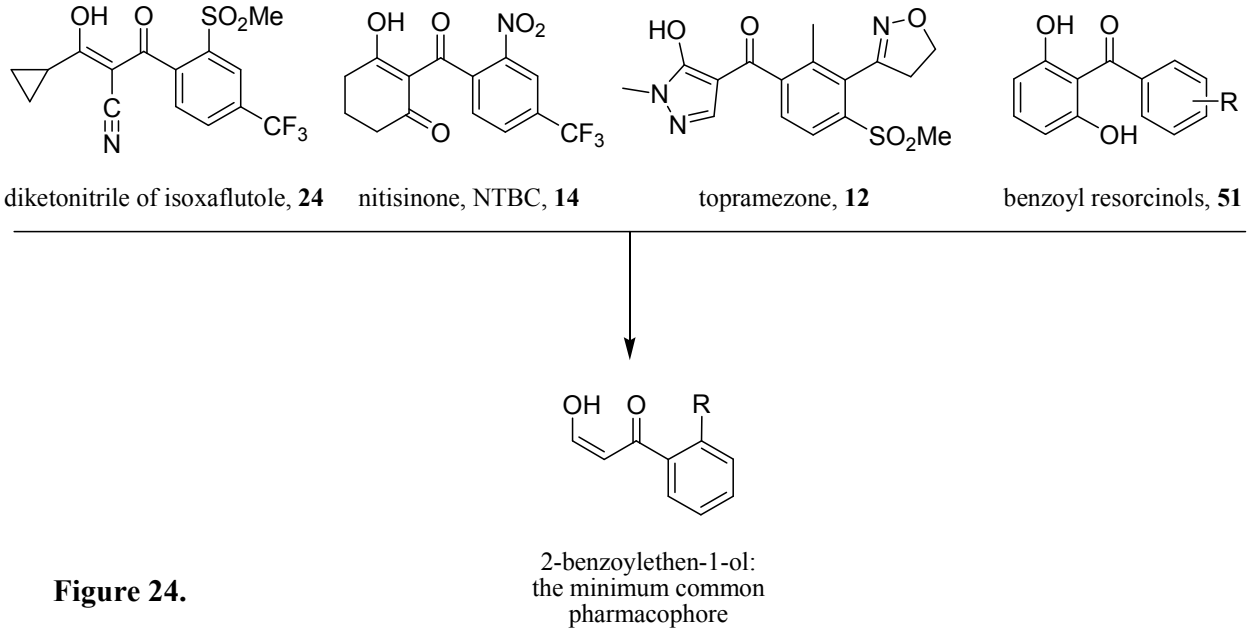

diketonitrile of isoxaflutole, **24** nitisinone, NTBC, **14** topramezone, **12** benzoyl resorcinols, **51**

2-benzoylethen-1-ol:
the minimum common
pharmacophore

Figure 24.

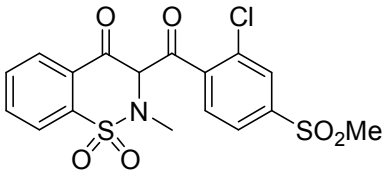

52: IC_{50} = 480 nM

Figure 25.

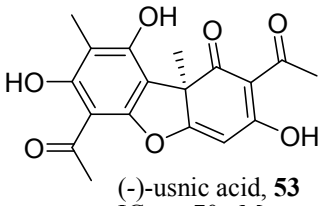

(-)-usnic acid, **53**
IC_{50} = 70 nM

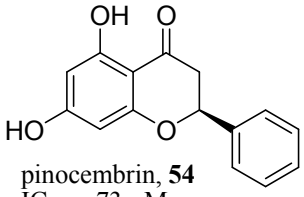

pinocembrin, **54**
IC_{50} = 73 μM

Figure 26.

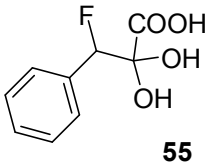

55
IC_{50} = 10 μM

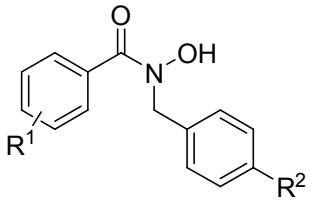

56: R^1 = 4-OMe, R^2 = H
57: R^1 = 4-OMe, R^2 = F
58: R^1 = 3-NH_2, R^2 = H

Figure 27.

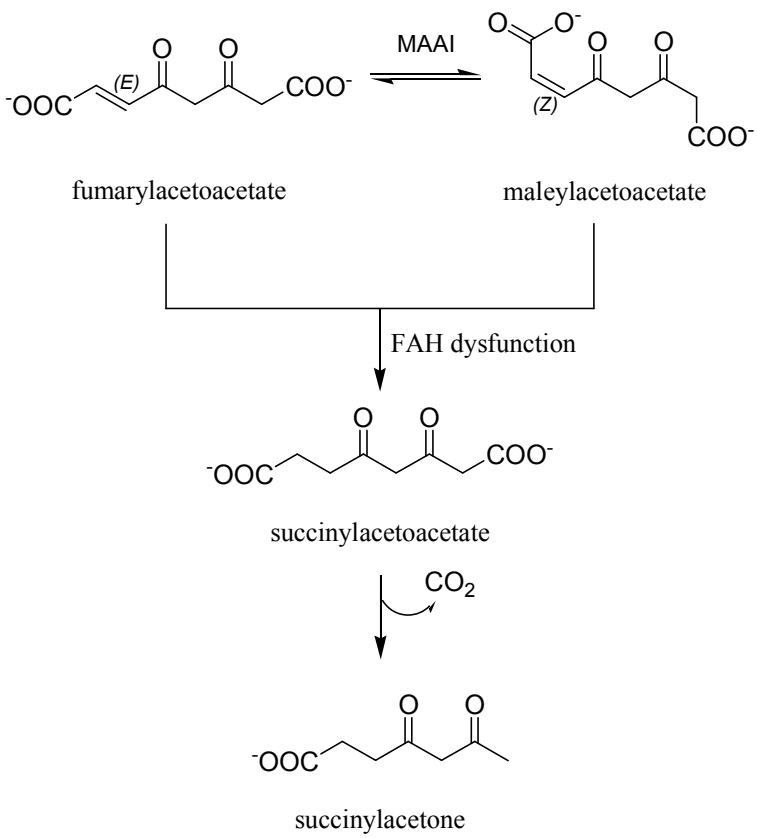

Figure 28.

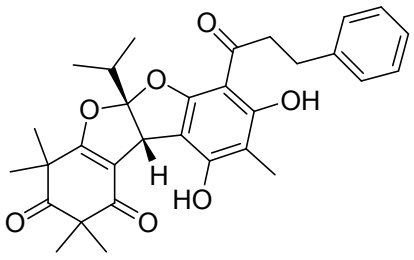

watsonianone B, **59**

Figure 29.

Figure captions

Figure 1. Schematic representation of the Phe/Tyr catabolic pathway.

Figure 2. Schematic representation of the chemical structure of the pyrazole derivatives 3 and 4.

Figure 3. Superposition of the complexes between HPPD (from *Rattus norvegicus*, green sticks, PDB entry 1SQI, and from *Arabidopsis thaliana*, red sticks, PDB entry 1TFZ) and the pyrazole inhibitor **3** (ball and stick notation). Amino acids of the binding site are all conserved and well superposed. Although a 29% amino acid identity, the root mean square deviation on 308 Cα atoms of the overall sequence is 1.2 Å. Two of the carbonyl moieties of the inhibitor are part of the coordination sphere of iron ion, together with the three catalytic residues (His and Glu). An aromatic cage of Phe residues accommodates the biphenyl moiety of the inhibitor. The *N*1-*t*Bu substituent is involved in hydrophobic interactions, while no hydrogen bonds are found between the ligand and HPPD. Picture was elaborated with Discovery Studio 3.0 Visualizer software, showing only a few amino acids of the binding site.

Figure 4. Superposition of the complexes between *At*HPPD and the pyrazole inhibitor **3** (green, PDB entry 1TFZ) or **4** (red, PDB entry 1TG5). The root mean square deviation on 362 Cα atoms of the overall sequence is 0.3 Å. The sole Phe403 undergoes a 115 degree rotation in the complex with **4**. Iron is coordinated by the usual carbonyl groups of the inhibitor and by the three amino acids of the binding site (His and Glu). Both the phenyl rings of the inhibitor interact by π-π stacking with Phe residues. Picture was elaborated with Discovery Studio 3.0 Visualizer software, showing only a few amino acids of the binding site.

Figure 5. Superposition of the complexes between HPPD (from *Arabidopsis thaliana*, green sticks, PDB entry 5CTO, and from *Streptomyces avermitilis*, red sticks, PDB entry 1T47) and the triketone inhibitor **14** (ball and stick notation). Residues of the binding site are all conserved and

superposed. The root mean square deviation on 314 Cα atoms of the overall sequence is 1.4 Å. The typical interactions between the keto-enol system, the iron ion, and the binding site amino acids were found. In addition to π-π stacking with Phe residues, a possible nitro-π stacking was also highlighted with Phe336 (1T47). Hydrophobic contacts involved the CF_3 group of the inhibitor. Picture was elaborated with Discovery Studio 3.0 Visualizer software, showing only a few amino acids of the binding site.

Figure 6. Proposed mechanism of the HPPD-catalyzed conversion of HPP (**1**) to HGA (**2**). Adapted from ref. 34 and 35.

Figure 7. Proposed mechanism of the HPPD-catalyzed production of small molecules alternative to **2**. Adapted from ref. 34 and 35.

Figure 8. Fate of **2** in plants.

Figure 9. Fate of **2** in patients with HGD disfunctions.

Figure 10. Structure of the most representative HPPD inhibitors belonging to the pyrazole and triketone classes.

Figure 11. Compound 23 and its active and inactive metabolites.

Figure 12. HPPD inhibitors from natural sources: **26** and its congeners.

Figure 13. Compound 29 and one by-product of its synthesis (benzoyl dimedone, **30**).

Figure 14. Summary of the major structure-activity relationships for triketone (cyclohexanedione) HPPD inhibitors.

Figure 15. Possible intramolecular cyclization from triketone to dihydroxanthone**.**

Figure 16. Keto-enol tautomerization of a representative triketone compound (**14**).

Figure 17. Importance of the triketone system for activity.

Figure 18. Benzoyl dimedone derivatives assayed in human fibroblasts.

Figure 19. Hybrid compounds by rational design.

Figure 20. Triketones bearing a quinazolindione, a quinoline, or a phenoxymethyl moiety as HPPD inhibitors.

Figure 21. Summary of the major structure-activity relationships for pyrazole HPPD inhibitors.

Figure 22. Pyrazolo-quinazolones and pyrazolo-benzimidazolones as HPPD inhibitors.

Figure 23. Rational design leading to isoxazole derivatives.

Figure 24. Hypothesis on the minimum common pharmacophore derived from representative examples of isoxazole, triketone, pyrazole, and resorcinol HPPD inhibitors.

Figure 25. Benzoyl-benzothiazines as HPPD inhibitors.

Figure 26. Additional HPPD inhibitors from natural sources.

Figure 27. HPPD inhibitors that mimic the substrate (hydrated derivatives of phenylpyruvic acid) or able to serve as cation chelators.

Figure 28. Metabolic production of toxic compounds due to FAH disfunctions in T1T patients.

Figure 29. A plant-derived syncarpic acid derivative with antiplasmodial activity.

Table of Contents graphic

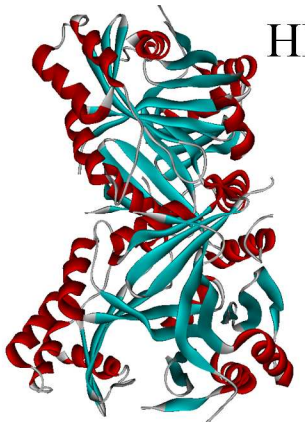

HPPD and its small molecule inhibitors in plants and animals

HPPD + triketones
HPPD + isoxazoles
HPPD + pyrazoles

↓

Herbicidal activity

Repositioning →

Cure for tyrosinemia type I
Clinical trials on alkaptonuria
Studies on tyrosinemia type II
Studies on hawkinsinuria
Studies on albinism type IB